



HAL
open science

Fast Protection of H.264/AVC by Selective Encryption of CAVLC and CABAC for I & P Frames

Zafar Shahid, Marc Chaumont, William Puech

► **To cite this version:**

Zafar Shahid, Marc Chaumont, William Puech. Fast Protection of H.264/AVC by Selective Encryption of CAVLC and CABAC for I & P Frames. *IEEE Transactions on Circuits and Systems for Video Technology*, 2011, 21 (5), pp.565-576. 10.1109/TCSVT.2013.2248588 . lirmm-00603198

HAL Id: lirmm-00603198

<https://hal-lirmm.ccsd.cnrs.fr/lirmm-00603198v1>

Submitted on 24 Jun 2011

HAL is a multi-disciplinary open access archive for the deposit and dissemination of scientific research documents, whether they are published or not. The documents may come from teaching and research institutions in France or abroad, or from public or private research centers.

L'archive ouverte pluridisciplinaire **HAL**, est destinée au dépôt et à la diffusion de documents scientifiques de niveau recherche, publiés ou non, émanant des établissements d'enseignement et de recherche français ou étrangers, des laboratoires publics ou privés.

Fast Protection of H.264/AVC by Selective Encryption of CAVLC and CABAC for I and P Frames

Zafar Shahid, Marc Chaumont, and William Puech, *Member, IEEE*

Abstract—This paper presents a novel method for the protection of bitstreams of state-of-the-art video codec H.264/AVC. The problem of selective encryption (SE) is addressed along with the compression in the entropy coding modules. H.264/AVC supports two types of entropy coding modules. Context-adaptive variable length coding (CAVLC) is supported in H.264/AVC baseline profile and context-adaptive binary arithmetic coding (CABAC) is supported in H.264/AVC main profile. SE is performed in both types of entropy coding modules of this video codec. For this purpose, in this paper the encryption step is done simultaneously with the entropy coding CAVLC or CABAC. SE is performed by using the advanced encryption standard (AES) algorithm with the cipher feedback mode on a subset of codewords/binstrings. For CAVLC, SE is performed on equal length codewords from a specific variable length coding table. In case of CABAC, it is done on equal length binstrings. In our scheme, entropy coding module serves the purpose of encryption cipher without affecting the coding efficiency of H.264/AVC by keeping exactly the same bitrate, generating completely compliant bitstream and utilizing negligible computational power. Owing to no escalation in bitrate, our encryption algorithm is better suited for real-time multimedia streaming over heterogeneous networks. It is perfect for playback on handheld devices because of negligible increase in processing power. Nine different benchmark video sequences containing different combinations of motion, texture, and objects are used for experimental evaluation of the proposed algorithm.

Index Terms—AES algorithm, CABAC, CAVLC, selective encryption, stream cipher, video security.

I. INTRODUCTION

WITH THE RAPID growth of processing power and network bandwidth, many multimedia applications have emerged in the recent past. As digital data can easily be copied and modified, the concern about its protection and authentication have surfaced. Digital rights management (DRM) has emerged as an important research field to protect the copyrighted multimedia data. DRM systems enforce the rights

Manuscript received December 9, 2009; revised May 18, 2010; accepted July 6, 2010. This work is supported in part by the VOODOO Project (2008–2011), which is a French national project of Agence Nationale de la Recherche (ANR), and the region of Languedoc Roussillon, France. This paper was recommended by Associate Editor M. Barni.

The authors are with the Laboratory of Informatics, Robotics, and Microelectronics, University of Montpellier II, Montpellier 34392, France (e-mail: zafar.shahid@lirmm.fr; marc.chaumont@lirmm.fr; william.puech@lirmm.fr).

Color versions of one or more of the figures in this paper are available online at <http://ieeexplore.ieee.org>.

Digital Object Identifier 10.1109/TCSVT.2011.2129090

of the multimedia property owners while ensuring the efficient rightful usage of such property.

Multimedia data requires either full encryption or selective encryption (SE) depending on the application requirements. For example, military and law enforcement applications require full encryption. Nevertheless, there is a large spectrum of applications that demands security on a lower level, as, e.g., that ensured by SE. SE encrypts part of the plaintext and has two main advantages. First, it reduces the computational requirements, since only a part of plaintext is encrypted [6]. Second, encrypted bitstream maintains the essential properties of the original bitstream [3]. SE just prevents abuse of the data. In the context of video, it refers to destroying the commercial value of video to a degree which prevents a pleasant viewing experience.

SE schemes based on H.264/AVC have been already presented on context-adaptive variable length coding (CAVLC) [29] and context-adaptive binary arithmetic coding (CABAC) [30]. These two previous methods fulfill real-time constraints by keeping the same bitrate and by generating completely compliant bitstream. In this paper, we have enhanced the previous proposed approaches by encryption of more syntax elements for CAVLC and extending it for P frames. Here, we have also used advanced encryption standard (AES) [7] in the cipher feedback (CFB) mode which is a stream cipher algorithm. Security of the proposed schemes has also been analyzed in detail.

The rest of this paper is organized as follows. In Section II, overview of H.264/AVC and AES algorithm is presented. We explain the whole system architecture of the proposed methods in Section III. Section IV contains experimental evaluation and security analysis. In Section V, we present the concluding remarks about the proposed schemes.

II. DESCRIPTION OF THE H.264/AVC-BASED VIDEO ENCRYPTION SYSTEM

A. Overview of H.264/AVC

H.264/AVC (also known as MPEG4 Part 10) [1] is state-of-the-art video coding standard of ITU-T and ISO/IEC. H.264/AVC has some additional features and outperforms previous video coding standards including MPEG2 and MPEG4 Part II [35]. We review the basic working of CAVLC in Section II-A1 and of CABAC in Section II-A2.

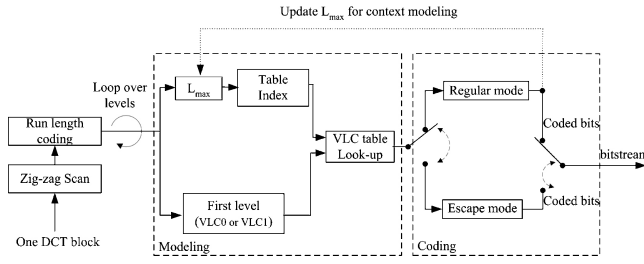


Fig. 1. Block diagram of level coding in CAVLC of H.264/AVC.

79 1) *CAVLC*: In CAVLC, run-length coding is performed
 80 first as it encodes levels and runs separately. CAVLC
 81 is designed to exploit the characteristics of NZs and works in
 82 several steps.

83 To adapt to the local statistical features of discrete cosine
 84 transform (DCT) coefficients, CAVLC uses seven fixed vari-
 85 able length coding (VLC) tables. For example, “2” will be
 86 coded as “010” using VLC1 table, while it will be coded as
 87 “1010” using VLC3 table. If magnitude of NZ lies within
 88 the range of that VLC table, it is coded by regular mode,
 89 otherwise escape mode is used. Adaptive nature is introduced
 90 by changing the table for the next NZ based on the magnitude
 91 of the current NZ as shown in Fig. 1. For the first NZ, VLC0
 92 table is used unless there are more than ten NZs and less than
 93 three trailing ones, in which case it is coded with VLC1 table.

94 2) *CABAC*: CABAC is designed to better exploit the
 95 characteristics of NZs as compared to CAVLC, consumes more
 96 processing, and offers about 10% better compression than
 97 CAVLC on average [22]. Run-length coding has been replaced
 98 by significant map coding which specifies the position of NZs
 99 in the 4×4 block. Binary arithmetic coding (BAC) module of
 100 CABAC uses many context models to encode NZs and context
 101 model for a specific NZ depends on recently coded NZs.

102 CABAC consists of multiple stages as shown in Fig. 2(a).
 103 First of all, binarization is done in which non-binary syntax
 104 elements are converted to binary form called binstrings which
 105 are more amenable to compression by BAC. Binary repre-
 106 sentation for a non-binary syntax element is done in such a
 107 way that it is close to minimum redundancy code. In CABAC,
 108 there are four basic code trees for binarization step, namely,
 109 the *unary* code, the *truncated unary* code, the *k*th order *Exp-*
 110 *Golomb* code (EGk), and the *fixed length* code as shown in
 111 Fig. 2(b).

112 For an unsigned integer value $x \geq 0$, the unary code consists
 113 of x 1s plus a terminating 0 bit. The truncated unary code is
 114 only defined for x with $0 \leq x \leq s$. For $x < s$, the code is
 115 given by the unary code, whereas for $x = s$ the terminating
 116 “0” bit is neglected. EGk is constructed by a concatenation
 117 of a prefix and a suffix parts and is suitable for binarization
 118 of syntax elements that represent prediction residuals. For a
 119 given unsigned integer value $x > 0$, the prefix part of the
 120 EGk binstring consists of a unary code corresponding to the
 121 length $l(x) = \lceil \log_2(\frac{x}{2k} + 1) \rceil$. The EGk suffix part is computed
 122 as the binary representation of $x + 2^k(1 - 2^{l(x)})$ using $k + l(x)$
 123 significant bits. Consequently for EGk binarization, the code
 124 length is $2l(x) + k + 1$. When $k = 0$, $2l(x) + k + 1 = 2l(x) + 1$.

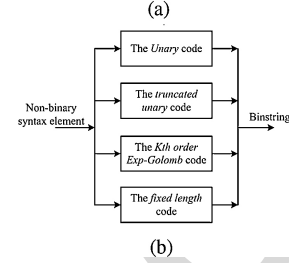
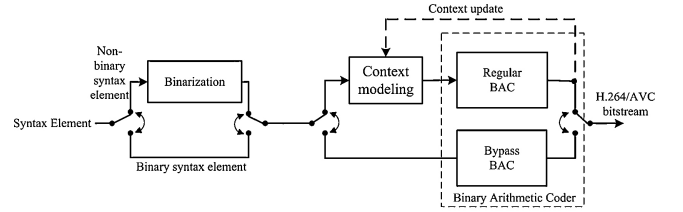


Fig. 2. (a) Block diagram of CABAC of H.264/AVC. (b) Binarization stage.

125 The fixed length code is applied to syntax elements with a
 126 nearly uniform distribution or to syntax elements, for which
 127 each bit in the fixed length code binstring represents a specific
 128 coding decision, e.g., coded block flag. Three syntax elements
 129 are binarized by concatenation of the basic code trees, namely,
 130 coded block pattern, NZ, and the motion vector difference
 131 (MVD). Binarization of absolute level of NZs is done by
 132 concatenation of truncated unary code and EG0. The truncated
 133 unary code constitutes the prefix part with cutoff value
 134 $S = 14$. Binarization and subsequent arithmetic coding process
 135 is applied to the syntax element $coeff_abs_value_minus1 =$
 136 $abs_level - 1$, since quantized transformed coefficients with
 137 zero magnitude are encoded using significant map. For MVD,
 138 binstring is constructed by concatenation of the truncated
 139 unary code and EG3. The truncated unary constitutes the prefix
 140 part with cutoff value $S = 9$. Suffix part of MVDs contains
 141 EG3 of $|MVD| - 9$ for $|MVD| > 9$ and sign bit.

B. AES Encryption Algorithm

142 The AES algorithm consists of a set of processing steps
 143 repeated for a number of iterations called rounds [7]. The
 144 number of rounds depends on the size of the key and the
 145 size of the data block. The number of rounds is nine, e.g.,
 146 if both the block and the key are 128 bits long. Given a
 147 sequence $\{X_1, X_2, \dots, X_n\}$ of bit plaintext blocks, each X_i
 148 is encrypted with the same secret key k producing the cipher-
 149 text blocks $\{Y_1, Y_2, \dots, Y_n\}$. To encipher a data block X_i
 150 in AES, you first perform an AddRoundKey step by XORing a
 151 subkey with the block. The incoming data and the key are added
 152 together in the first AddRoundKey step. Afterward, it follows
 153 the round operation. Each regular round operation involves
 154 four steps which are SubBytes, ShiftRows, MixColumns, and
 155 AddRoundKey. Before producing the final ciphered data Y_i ,
 156 the AES performs an extra final routine that is composed of
 157 SubBytes, ShiftRows, and AddRoundKey steps.

158 The AES algorithm can support several cipher modes:
 159 electronic code book (ECB), cipher block chaining, output
 160 feedback (OFB), CFB, and counter (CTR) [31]. The ECB
 161 mode is actually the basic AES algorithm. In CFB mode, as
 162

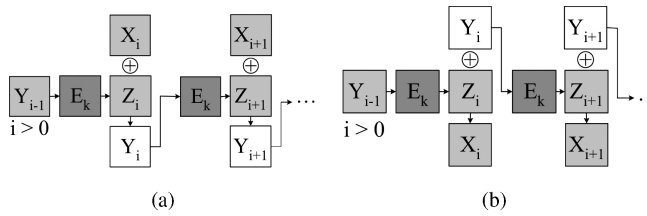


Fig. 3. CFB stream cipher. (a) Encryption. (b) Decryption.

163 shown in Fig. 3, the keystream element Z_i is generated and
 164 the ciphertext block Y_i is produced as follows:

$$\begin{cases} Z_i = E_k(Y_{i-1}), \text{ for } i \geq 1 \\ Y_i = X_i \oplus Z_i \end{cases} \quad (1)$$

165 where \oplus is the XOR operator.

166 Although AES is a block cipher, in the OFB, CFB, and
 167 CTR modes it operates as a stream cipher.

168 C. SE of Image and Video

169 SE is a technique aiming to save computational time or to
 170 enable new system functionalities by only encrypting a portion
 171 of a compressed bitstream while still achieving adequate
 172 security [18]. SE as well as partial encryption (PE) are applied
 173 only on certain parts of the bitstream. In the decoding stage,
 174 both the encrypted and the non-encrypted information should
 175 be appropriately identified and displayed [6], [21], [26]. The
 176 copyright protection of the multimedia content is a required
 177 feature for DRM systems. The technical challenges posed
 178 by such systems are high and previous approaches have not
 179 entirely succeeded in tackling them [17].

180 In [32], Tang proposed a technique called zigzag permutation
 181 applicable to DCT-based image and video codecs. On one
 182 hand, this method provides a certain level of confidentiality,
 183 while on the other hand, it increases the overall bitrate.
 184 For image, several SE techniques have been proposed in
 185 the literature. In [8], Droogenbroeck and Benedett proposed
 186 a technique for encryption of JPEG images. It encrypts a
 187 selected number of AC coefficients. The DC coefficients are
 188 not ciphered since they carry important visual information
 189 and they are highly predictable. In spite of the constancy
 190 in the bitrate while preserving the bitstream compliance, the
 191 compression and the encryption process are separated and
 192 consequently the computational complexity is increased.

193 The AES [7] has been used for SE of image and video in
 194 the literature. The AES was applied on the Haar discrete
 195 wavelet transform compressed images in [23]. The encryption
 196 of color images in the wavelet transform has been addressed
 197 in [21]. In this approach, the encryption is performed on the
 198 resulting wavelet code bits. In [25], SE was performed on color
 199 JPEG images by selectively encrypting only *luma* component
 200 using AES cipher. The protection rights of individuals and the
 201 privacy of certain moving objects in the context of security
 202 surveillance systems using viewer generated masking and the
 203 AES encryption standard has been addressed in [37].

204 Combining PE and image/video compression using the set
 205 partitioning in hierarchical trees was used in [6]. Nevertheless,
 206 this approach requires a significant computational complexity.

207 A method that does not require significant processing time and
 208 which operates directly on the bit planes of the image was
 209 proposed in [19]. The robustness of partially encrypted videos
 210 to attacks which exploit the information from non-encrypted
 211 bits together with the availability of side information was
 212 studied in [27]. Fisch *et al.* [10] proposed a scalable encryption
 213 method for a DCT-coded visual data wherein the data are
 214 organized in a scalable bitstream form. These bitstreams are
 215 constructed with the DC and some AC coefficients of each
 216 block which are then arranged in layers according to their
 217 visual importance, and PE process is applied over these layers.

218 For video, there are several SE techniques for different
 219 video codecs presented in the literature. SE of MPEG4 video
 220 standard was studied in [34] wherein data encryption standard
 221 was used to encrypt fixed length and variable length codes. In
 222 this approach, the encrypted bitstream is completely compliant
 223 with MPEG4 bitstream format but it increases the bitrate.
 224 A tradeoff has to be made among complexity, security, and
 225 the bit overhead. In [38], SE of MPEG4 video standard is
 226 proposed by doing frequency domain selective scrambling,
 227 DCT block shuffling, and rotation. This scheme is very easy to
 228 perform but its limitation is its bitrate overhead. SE of region
 229 of interest (ROI) of MPEG4 video has been presented in [9].
 230 It performs SE by pseudo randomly inverting sign of DCT
 231 coefficients in ROI. SE of H.264/AVC has been studied in [15]
 232 wherein encryption has been carried out in some fields like
 233 intra-prediction mode, residual data, inter-prediction mode,
 234 and motion vectors. A scheme for commutative encryption
 235 and watermarking of H.264/AVC is presented in [16]. Here,
 236 SE of some macroblock (MB) header fields is combined
 237 with watermarking of magnitude of DCT coefficients. This
 238 scheme presents a watermarking solution in encrypted domain
 239 without exposing video content. The limitation of techniques
 240 proposed in [15] and [16] is that they are not format compliant.
 241 Encryption for H.264/AVC has been discussed in [5] wherein
 242 they do permutations of the pixels of MBs which are in ROI.
 243 The drawback of this scheme is that bitrate increases as the
 244 size of the ROI increases. This is due to change in the statistics
 245 of ROI as it is no more a slow varying region which is
 246 the basic assumption for video signals. SE of H.264/AVC at
 247 network abstraction layer (NAL) has been proposed in [14].
 248 Important NAL units, namely, instantaneous decoding refresh
 249 picture, sequence parameter set, and picture parameter set are
 250 encrypted with a stream cipher. The limitation of this scheme
 251 is that it is not format compliant and cannot be parsed even at
 252 frame level. SE of H.264/AVC using AES has been proposed
 253 in [2]. In this scheme, encryption of I frame is performed,
 254 since P and B frame are not significant without I frames. This
 255 scheme is not format compliant.

256 The use of general entropy coder as encryption cipher
 257 using statistical models has been studied in the literature
 258 in [36]. It encrypts by using different Huffman tables for
 259 different input symbols. The tables, as well as the order
 260 in which they are used, are kept secret. This technique is
 261 vulnerable to known plaintext attacks as explained in [12].
 262 Key-based interval splitting of arithmetic coding (KSAC) has
 263 used an approach [13] wherein intervals are partitioned in each
 264 iteration of arithmetic coding. Secret key is used to decide

265 how the interval will be partitioned. Number of subintervals in
 266 which an interval is divided should be kept small as it increases
 267 the bitrate of bitstream. Randomized arithmetic coding [11]
 268 is aimed at arithmetic coding but instead of partitioning of
 269 intervals like in KSAC, secret key is used to scramble the
 270 order of intervals. The limitation of these entropy coding-based
 271 techniques is that encrypted bitstream is not format compliant.
 272 Moreover, these techniques require lot of processing power.

273 In the context of DRM systems, our paper addresses
 274 the simultaneous SE and compression for state-of-the-art
 275 H.264/AVC. The encrypted bitstream is format compliant with
 276 absolutely no escalation in bitrate. Furthermore, it does not
 277 require lot of processing power for encryption and decryption.
 278 In Section III, we describe our proposed approaches to
 279 apply SE and H.264/AVC compression in video sequences,
 280 simultaneously.

281 III. PROPOSED SE SCHEMES

282 Our approach consists of SE during the entropy coding
 283 stage of H.264/AVC. In baseline profile, SE is performed in
 284 CAVLC entropy coding stage (SE-CAVLC). While in main
 285 profile, it is performed in CABAC entropy coding stage (SE-
 286 CABAC). In SE of video, encrypted bitstream compliance is a
 287 required feature for some direct operations such as displaying,
 288 time seeking, and browsing. Encrypted bitstream will be
 289 compliant and fulfills real-time constraints if the following
 290 three conditions are fulfilled.

- 291 1) To keep the bitrate of encrypted bitstream same as the
- 292 original bitstream, encrypted codewords/binstrings must
- 293 have the same size as the original codewords/binstrings.
- 294 2) The encrypted codewords/binstrings must be valid so
- 295 that they may be decoded by entropy decoder.
- 296 3) The decoded value of syntax element from encrypted
- 297 codewords/binstrings must stay in the valid range for
- 298 that syntax element. Any syntax element which is used
- 299 for prediction of neighboring MBs should not be encr-
- 300 ypted. Otherwise, the drift in the value of syntax ele-
- 301 ment will keep on increasing and after a few iterations,
- 302 value of syntax element will fall outside the valid range
- 303 and bitstream will be no more decodable.

304 In each MB, header information is encoded first, which is
 305 followed by the encoding of MB data. To keep the bitstream
 306 compliant, we cannot encrypt MB header, since it is used
 307 for prediction of future MBs. MB data contains NZs and
 308 can be encrypted. A MB is further divided into 16 blocks of
 309 4×4 pixels to be processed by integer transform module. The
 310 coded block pattern is a syntax element used to indicate which
 311 8×8 blocks within a MB contain NZs. The *macroblock mode*
 312 (MBmode) is used to indicate whether a MB is *skipped* or not.
 313 If MB is not *skipped*, then MBmode indicates the prediction
 314 method for a specific MB. For a 4×4 block inside MB, if
 315 coded block pattern and MBmode are set, it indicates that this
 316 block is encoded. Inside 4×4 block, coded block flag is the
 317 syntax element used to indicate whether it contains NZs or not.
 318 It is encoded first. If it is zero, no further data is transmitted;
 319 otherwise, it is followed by encoding of significant map in
 320 case of CABAC. Finally, the absolute value of each NZ and

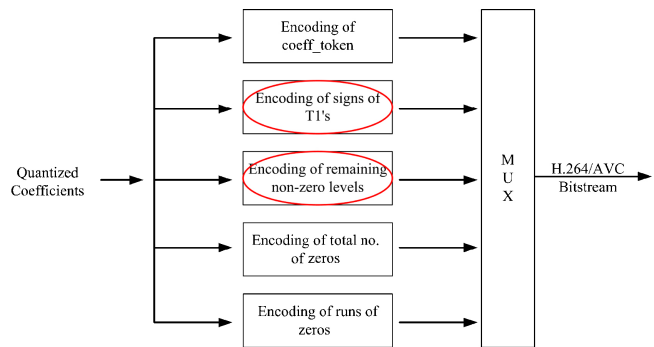


Fig. 4. Block diagram of CAVLC of H.264/AVC. Encircled syntax elements are used for SE-CAVLC.

321 its sign are encoded. Similar to MB header, header of 4×4
 322 block which includes coded block flag and significant map,
 323 should not be encrypted for the sake of bitstream compliance.
 324 Available encryption space (ES) which fulfills the above-
 325 mentioned conditions for SE-CAVLC and SE-CABAC is pre-
 326 sented in Sections III-A and III-B, respectively. Encryption
 327 and decryption of the protected bitstream are presented in
 328 Sections III-C and III-D, respectively.

329 A. ES for SE-CAVLC

330 In CAVLC, five syntax elements are used to code levels
 331 and runs as shown in Fig. 4. NZs are coded by three syntax
 332 elements, namely, *coeff_token*, signs of trailing ones, and
 333 remaining nonzero levels. Zeros are coded by two syntax
 334 elements, namely, total number of zeros and runs of zeros.
 335 A single syntax element, namely, *coeff_token* is used to code
 336 total NZs and number of trailing ones. It is followed by coding
 337 of signs of trailing ones (T1s). Remaining NZs are then coded
 338 using seven VLC look-up tables either by regular mode or by
 339 escape mode as explained in Section II-A1. They are mapped
 340 to some code from a specific VLC look-up table.

341 To keep the bitstream compliant, we cannot encrypt *coeff_*
 342 *token*, total number of zeros, and runs of zeros. Two
 343 syntax elements fulfill the above-mentioned conditions for
 344 encryptions. First is signs of trailing ones. Second is sign and
 345 magnitude of remaining NZs, both in regular and escape mode.
 346 For the sake of same bitrate, ES of SE-CAVLC consists of
 347 only those NZs whose VLC codewords have the same length.
 348 CAVLC uses multiple VLC tables with some threshold for
 349 incrementing the table as given in (2). Since the threshold for
 350 a specific table is highest possible value possible with that
 351 codeword length (this is the case when all the suffix bits of
 352 the codeword are 1), magnitude of encrypted NZ is such that
 353 VLC table transition is not affected. VLC codes, having same
 354 code length, constitute the ES. For VLC n table, ES is 2^n as
 355 given in (3). For table VLC0, every NZ has different codeword
 356 length, consequently we cannot encrypt the NZs in this table
 357 as follows:

$$TH[0 \dots 6] = (0, 2, 3, 6, 12, 24, 48, \infty). \quad (2)$$

$$ES[0 \dots 6] = (1, 2, 4, 8, 16, 32, 64, \infty). \quad (3)$$



Fig. 5. SE of binstrings in SE-CABAC.

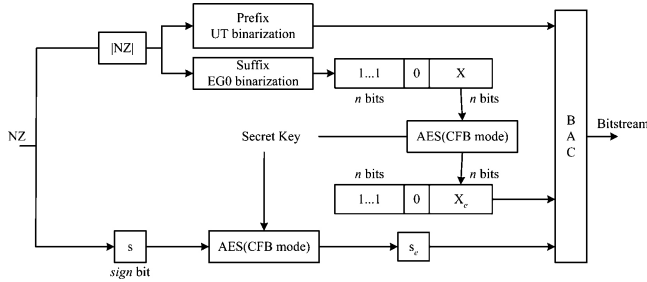


Fig. 6. Encryption process for NZs and their signs in CABAC of H.264/AVC.

B. ES for SE-CABAC

The main difference between SE-CAVLC and SE-CABAC is that in SE-CABAC, SE is not performed on CABAC bitstream. Rather it is performed on binstrings which are input to BAC as shown in Fig. 5. Among all the four binarization techniques, the unary and truncated unary codes have different code lengths for each input value as explained in Section II-A2. They do not fulfill the first condition and their encryption will change the bitrate of bitstream. Suffix of EGk and the fixed length code can be encrypted while keeping the bitrate unchanged. EGk is used for binarization of absolute value of levels and MVDs. Number of MVD binstrings have the same length and hence, first and second conditions are fulfilled. But owing to the fact that MVDs are part of MB header and are used for prediction of future motion vectors, their encryption does not fulfill third condition and their encryption makes the bitstream non-compliant. To conclude, the syntax elements which fulfill the criteria for encryption of H.264/AVC compliant bitstream are suffix of EG0 and sign bits of levels. Hence, for each NZ with $|NZ| > 14$, encryption is performed on $l(x)$ of EG0. It is followed by encryption of syntax element *coeff_sign_flag* which represents sign of levels of all nonzero levels. The fixed length code is used for binarization of syntax elements which belong to MB header and cannot be encrypted.

To keep the bitrate intact, ES for SE-CABAC consists of only those NZs whose EG0 binstrings have the same length as shown in Fig. 6. EG0 codes, having same code length, constitute the ES and it depends upon $\|NZ\|$. The ES is $2^{\log_2(n+1)}$ where n is the maximum possible value by suffix bits of EG0, i.e., when all the bits in suffix are 1.

C. SE of NZs in the Entropy Coding Stage of H.264/AVC

Let us consider $Y_i = X_i \oplus E_k(Y_{i-1})$ as the notation for the encryption of a n bit block X_i , using the secret key k with the AES cipher in CFB mode as given by (1), and performed as described in the scheme from Fig. 3. We have chosen to use this mode in order to keep the original compression rate. Indeed, with the CFB mode for each block, the size of the encrypted data Y_i can be exactly the same one as

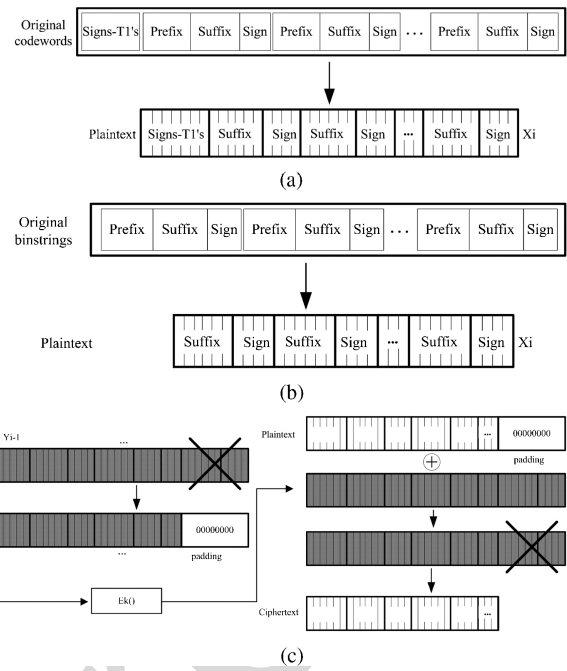


Fig. 7. (a) CAVLC plaintext. (b) CABAC plaintext. (c) Proposed SE scheme.

the size of the plaintext X_i . In this mode, the code from the previously encrypted block is used to encrypt the current one as shown in Fig. 3. The three stages of the proposed algorithm are the construction of the plaintext X_i , described in Section III-C1, the encryption of X_i to create Y_i which is provided in Section III-C2, and the substitution of the original codeword/binstring with the encrypted information, which is explained in Section III-C3. The overview of the proposed SE method is provided in Fig. 7.

1) *Construction of Plaintext*: As slices are independent coding units, SE should be performed on them independently. In case of SE-CAVLC, the plaintext is created by copying the encrypt-able bits from CAVLC bitstream to the vector X_i until either X_i is completely filled or slice-boundary comes as shown in Fig. 7(a). Let C , the length of the vector X_i , is 128. In case of SE-CABAC, we perform SE before BAC as shown in Fig. 7(b). In that case, we transform the non-binary syntax elements to binstrings through process of binarization and at the same time we fill the X_i with encrypted bits until either the vector X_i is completely filled or the slice boundary comes. The binarization of many syntax elements at the same time also makes the CABAC coding faster and increases its throughput [39]. Let $L(X_i)$ be the length up to which vector X_i is filled. In case of slice boundary, if $L(X_i) < C$, we apply a padding function $p(j) = 0$, where $j \in \{L(X_i) + 1, \dots, C\}$, to fill in the vector X_i with zeros up to C bits. Historically, padding was used to increase the security of the encryption, but in here it is used for rather technical reasons [28].

2) *Encryption of the Plaintext with AES in the CFB Mode*: In the encryption step with AES in the CFB mode, the previous encrypted block Y_{i-1} is used as the input of the AES algorithm in order to create Z_i . Then, the current plaintext X_i is XORed with Z_i in order to generate the encrypted text Y_i as given by (1). For the initialization, the initialization vector (IV)

is created from the secret key k according to the following strategy. The secret key k is used as the seed of the pseudo random number generator (PRNG). First, the secret key k is divided into 8 bits (byte) sequences. The PRNG produces a random number for each byte component of the key that defines the order of IV formation. Then, we substitute Y_0 with the IV, and Y_0 is used in AES to produce Z_1 . As illustrated in Fig. 7(c), with the CFB mode of the AES algorithm, the generation of the keystream Z_i depends on the previous encrypted block Y_{i-1} . Consequently, if two plaintexts are identical $X_i = X_j$ in the CFB mode, then always the two corresponding encrypted blocks are different, $Y_i \neq Y_j$.

3) *Substitution of the Original Bitstream*: The third step is the substitution of the original Y_i by the encrypted Y_i . For SE-CAVLC, CAVLC bitstream is accessed in sequential order as in the first step (construction of the plaintext X_i). Given the length in bits of each amplitude (S_n, S_{n-1}, \dots, S_1), we start substituting the original bits in the bitstream by the corresponding parts of Y_i as shown in Fig. 7. For SE-CABAC, binstrings are accessed in sequential order and we start substituting the original bits in them by the corresponding parts of Y_i as shown in Fig. 7. In case of slice boundaries, the total quantity of replaced bits is $L(X_i)$ and consequently we do not necessarily use all the bits of Y_i .

D. Decryption Process

The decryption process in the CFB mode works as follows. The previous block Y_{i-1} is used as the input to the AES algorithm in order to generate Z_i . By knowing the secret key k , we apply the same function $E_k(\cdot)$ as that used in the encryption stage. The difference is that the input of this process is now the ciphered vector. In case of SE-CAVLC, the ciphered vector is accessed in the sequential way in order to construct the plaintext Y_{i-1} which is then used in the AES to generate the keystream Z_i . The keystream Z_i is then XORed with the current block Y_i to generate X_i , as shown in Fig. 3(b). For SE-CAVLC, the resulting plaintext vector is split into segments in order to substitute the signs of trailing ones and suffixes (S_n, S_{n-1}, \dots, S_1) in the ciphered bitstream and to generate the original CAVLC bitstream. Afterward, we apply the entropy decoding and retrieve the quantized DCT coefficients. After the inverse quantization and the inverse DCT we get the decrypted and decoded video frame. In case of SE-CABAC, the difference is that binary arithmetic decoder is used to transform the SE-CABAC bitstream to encrypted binstrings which are then accessed to make the plaintext Y_{i-1} . The plaintext is decrypted and substituted back to generate original binstrings. They are then passed through inverse binarization, inverse quantization, and inverse DCT steps to get the decrypted and decoded video frame.

IV. EXPERIMENTAL RESULTS

In this section, we analyze the results for SE-CAVLC and SE-CABAC. We have used the reference implementation of H.264 JSVM 10.2 in AVC mode for video sequences in quarter common intermediate format (QCIF) and SD resolution. For the experimental results, nine benchmark video sequences

have been used for the analysis in QCIF format. Each of them represents different combinations of motion (fast/slow, pan/zoom/rotation), color (bright/dull), contrast (high/low), and objects (vehicle, buildings, people). The video sequences *Bus*, *City*, and *Foreman* contain camera motion while *Football* and *Soccer* contain camera panning and zooming along with object motion and texture in background. The video sequences *Harbour* and *Ice* contain high luminance images with smooth motion. *Mobile* sequence contains a complex still background and foreground motion.

In Section IV-A, we present an analysis of joint SE and H.264/AVC compression while in Section IV-B, we compare PSNR and quality when applying SE only on I frames and on I+P frames. In Section IV-C, security analysis, showing the efficiency of the proposed method, is developed.

A. Analysis of Joint SE and H.264/AVC Compression

We have applied simultaneously our SE and H.264/AVC compression as described in Section III, on all the benchmark video sequences. SE-CAVLC and SE-CABAC impart some characteristics to the bitstream. In spatial domain, SE video gets flat regions and change in pixel values mostly occur on MB boundaries. In temporal domain, *luma* and *chroma* values rise up to maximum limit and then come back to minimum values. This cycle keeps on repeating. Owing to this phenomenon, the pixel values change drastically in temporal domain. Lot of transitions are observed in values of color and brightness.

In a first set of experiments, we have analyzed the available ES in H.264/AVC bitstreams for both of SE-CAVLC and SE-CABAC. ES is defined as percentage of total bitstream size. MBs that contain many details and texture will have lot of NZs and, consequently, will be strongly encrypted. On the contrary, the homogeneous MBs, i.e., blocks that contain series of identical pixels, are less ciphered because they contain a lot of null coefficients which are represented by runs in CAVLC and by significant map in CABAC. In Table I, we provide ES for SE-CAVLC and SE-CABAC for different benchmark video sequences for quantization parameter (QP) value 18. While in Table II, ES for various QP values is shown for *Foreman* video sequence. Here the average number of bits available for SE per MB are also provided. One can note that ES is inversely proportional to QP value. When QP value is higher and implicitly the video compression is higher, we are able to encrypt fewer bits in the compressed frame. This is due to the fact that H.264/AVC has lesser number of NZs at higher QP values. From both these tables, it is evident that more ES is available for SE-CAVLC as compared to SE-CABAC. But ES is more affected by change in QP values for SE-CAVLC as compared to SE-CABAC. For example, for *Foreman* video sequence, ES varies from 28.55% to 6.70% for SE-CAVLC when QP varies from 12 to 42. For the same QP range, the change in ES for SE-CABAC is from 19.97% to 9.46% as shown in Table II. From Tables I and II, since PSNR of original H.264/AVC are very similar for both CAVLC and CABAC, in the rest of this section for the sake of comparison, we list only PSNR of CAVLC bitstreams.

TABLE I
ANALYSIS OF ES FOR SE FOR DIFFERENT BENCHMARK VIDEO
SEQUENCES AT QP VALUE 18

Sequence	SE-CAVLC		SE-CABAC	
	PSNR (dB)	ES (%)	PSNR (dB)	ES (%)
<i>Bus</i>	44.25	31.05	44.24	19.93
<i>City</i>	44.29	26.41	44.27	19.79
<i>Crew</i>	44.82	20.66	44.81	18.97
<i>Football</i>	44.61	25.33	44.59	19.45
<i>Foreman</i>	44.38	22.76	44.36	18.72
<i>Harbor</i>	44.10	30.49	44.09	20.01
<i>Ice</i>	46.47	24.64	46.46	17.72
<i>Mobile</i>	44.44	36.17	44.43	19.80
<i>Soccer</i>	44.27	23.42	44.21	19.94

TABLE II
ANALYSIS OF ES FOR SE OVER WHOLE RANGE OF QP VALUES FOR
Foreman VIDEO SEQUENCE

QP	SE-CAVLC		SE-CABAC	
	PSNR (dB)	ES (%)	PSNR (dB)	ES (%)
12	50.07	28.55	50.05	19.97
18	44.38	22.76	44.36	18.72
24	39.43	17.13	39.42	17.61
30	35.08	13.24	35.08	15.65
36	31.04	9.88	31.06	12.22
42	27.23	6.70	27.35	9.46

TABLE III
ANALYSIS OF INCREASE IN PROCESSING POWER FOR SE-CAVLC AND
SE-CABAC AT QP VALUE 18

Sequence	SE-CAVLC				SE-CABAC			
	Encoder		Decoder		Encoder		Decoder	
	I (%)	I+P (%)	I (%)	I+P (%)	I (%)	I+P (%)	I (%)	I+P (%)
<i>Bus</i>	0.69	0.31	3.77	2.7	0.57	0.25	3.37	2.3
<i>City</i>	0.5	0.26	3.36	2.4	0.44	0.23	3.06	2.1
<i>Crew</i>	0.31	0.15	2.52	1.5	0.29	0.14	2.22	1.2
<i>Football</i>	0.41	0.23	3.46	2.4	0.31	0.18	3.26	2.2
<i>Foreman</i>	0.47	0.23	3.19	2.2	0.41	0.20	2.99	2.0
<i>Harbor</i>	0.55	0.30	3.65	2.7	0.47	0.26	3.25	2.3
<i>Ice</i>	0.41	0.21	3.16	2.1	0.33	0.17	2.96	1.9
<i>Mobile</i>	0.76	0.35	4.33	3.3	0.72	0.33	4.03	3.0
<i>Soccer</i>	0.44	0.21	3.17	2.2	0.38	0.18	2.87	1.9

Table III gives a detailed overview of the required processing power for I and I+P video sequences at QP value 18. *Intra period* has been set 10 for I+P video sequences. One can observe that increase in computation time for encoder is less than 0.4% for both of SE-CAVLC and SE-CABAC while it is below than 3% for decoder for I+P sequence.

Fig. 8(a) and (b) shows the framewise analysis of increase in processing power for SE-CABAC at QP value 18 for *Foreman*. For experimentation, 2.1 GHz Intel Core 2 Duo T8100 machine with 3072 MB random access memory has been used. For I+P sequence encoding of 100 frames with *intra period* 10, it took 4372.5 s and 4381.3 s for CABAC and SE-CABAC, respectively. While it took 2.005 s and 2.045 s for CABAC and SE-CABAC decoding. It is a negligible increase in processing power and can be managed well even by handheld devices. It is important to note that increase in processing power of SE-

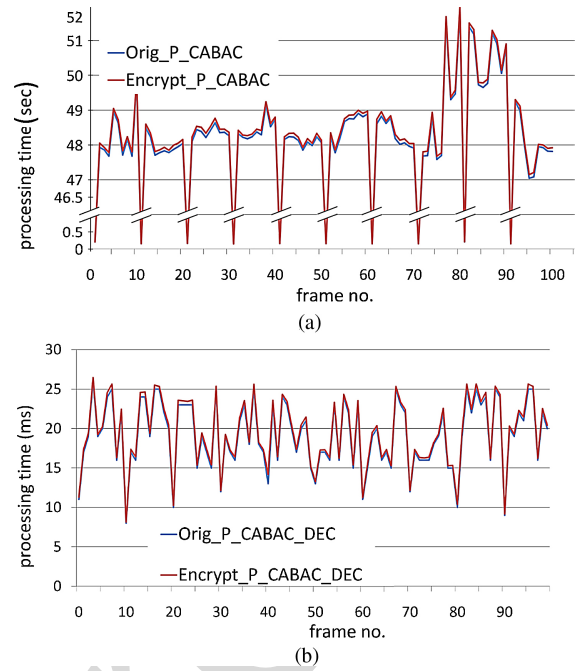


Fig. 8. Framewise time taken by SE-CABAC of *Foreman* video sequence for I+P frames at QP value 18 with *intra period* 10 during (a) encoding and (b) decoding.

CABAC is less than SE-CAVLC owing to two reasons. First, ES of SE-CABAC is lesser than that of SE-CAVLC as shown in Tables I and II. Second, CABAC takes lot more processing power than CAVLC. So increase in processing power because of encryption will be lower in terms of percentage. Thus, SE-CAVLC and SE-CABAC is possible in real-time along with compression.

B. PSNR and Quality of SE-CAVLC and SE-CABAC for I Frames and I+P Frames

Peak signal to noise ratio (PSNR) is widely used objective video quality metric. However, it does not perfectly correlate with a perceived visual quality due to nonlinear behavior of human visual system. Structural similarity index (SSIM) [33] takes into account the structural distortion measurement, since human vision system is highly specialized in extracting structural information from the viewing field. SSIM has a better correlation to the subjective impression. SSIM ranges from -1 to 1 . SSIM is 1 when both the images are the same. To present the visual protection of encrypted video sequences, PSNR and SSIM of I and I+P frames are presented.

1) *I Frames*: To demonstrate the efficiency of our proposed scheme, we have compressed 100 I frames of each sequence at 30f/s. Figs. 9 and 10 show the encrypted first frame of *Foreman* video sequence at different QP values for SE-CAVLC and SE-CABAC, respectively. In H.264/AVC, blocks on the top array are predicted only from left while blocks on left are always predicted from top. Owing to this prediction, a band having width of 8 pixels at top of video frames can be observed for both of SE-CAVLC and SE-CABAC while this band has width of 4 pixels on left of video frames as shown in Figs. 9 and 10. The average PSNR values of *Foreman* is

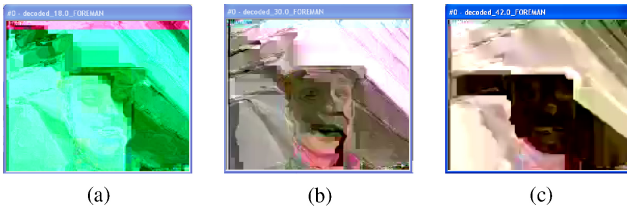


Fig. 9. Decoding of SE-CAVLC frame #1 of *Foreman* sequence with QP value equal to (a) 18, (b) 30, and (c) 42.

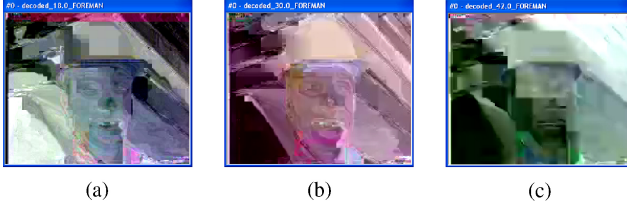


Fig. 10. Decoding of SE-CABAC frame #1 of *Foreman* sequence with QP value equal to (a) 18, (b) 30, and (c) 42.

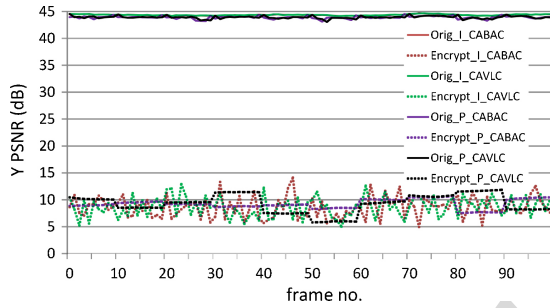


Fig. 11. Framewise PSNR of I and I+P frames for *Foreman* for SE-CAVLC and SE-CABAC at QP value 18.

TABLE IV
PSNR COMPARISON FOR I FRAMES WITHOUT ENCRYPTION AND WITH SE FOR *Foreman* AT DIFFERENT QP VALUES

QP	PSNR (Y) (dB)			PSNR (U) (dB)			PSNR (V) (dB)		
	ORIG	SE	SE	ORIG	SE	SE	ORIG	SE	SE
		CAVLC	CABAC		CAVLC	CABAC		CAVLC	CABAC
12	50.1	8.6	8.4	50.0	19.8	24.1	50.8	9.6	22.6
18	44.4	8.7	8.6	45.7	24.1	24.4	47.6	10.2	22.1
24	39.4	8.7	8.7	41.9	26.4	24.4	44.2	24.9	22.8
30	35.1	9.4	8.7	39.8	27.4	24.6	41.4	25.4	23.6
36	31.0	9.4	8.5	37.7	28.1	24.9	38.6	24.8	23.2
42	27.2	9.4	8.7	36.2	25.5	24.9	36.9	24.6	24.0

TABLE V
PSNR COMPARISON FOR I FRAMES WITHOUT ENCRYPTION AND WITH SE AT QP VALUE 18

Sequence	PSNR (Y) (dB)			PSNR (U) (dB)			PSNR (V) (dB)		
	ORIG	SE	SE	ORIG	SE	SE	ORIG	SE	SE
		CAVLC	CABAC		CAVLC	CABAC		CAVLC	CABAC
<i>Bus</i>	44.2	7.9	8.2	45.2	26.8	25.0	46.6	26.6	27.2
<i>City</i>	44.3	10.9	11.2	45.8	31.9	30.3	46.8	33.5	31.8
<i>Crew</i>	44.8	9.0	9.9	45.8	24.0	23.4	45.7	19.7	19.8
<i>Football</i>	44.6	11.5	11.5	45.8	14.9	14.4	46.0	24.3	23.6
<i>Foreman</i>	44.4	8.7	8.6	45.7	24.1	24.4	47.6	10.2	22.1
<i>Harbor</i>	44.1	9.2	9.5	45.6	27.1	24.6	46.7	33.2	31.3
<i>Ice</i>	46.5	10.6	10.4	48.8	24.3	25.6	49.3	16.9	20.4
<i>Mobile</i>	44.4	8.3	8.3	44.1	10.4	13.1	44.1	9.6	11.0
<i>Soccer</i>	44.3	9.3	10.6	46.6	22.1	19.7	47.9	28.2	24.4
Average	44.6	9.5	9.8	46.0	22.8	22.3	46.7	22.5	23.5

TABLE VI
PSNR COMPARISON FOR I FRAMES WITHOUT ENCRYPTION AND WITH SE AT QP VALUE 18 (SD RESOLUTION)

Sequence	PSNR (Y) (dB)			PSNR (U) (dB)			PSNR (V) (dB)		
	ORIG	SE	SE	ORIG	SE	SE	ORIG	SE	SE
		CAVLC	CABAC		CAVLC	CABAC		CAVLC	CABAC
<i>City</i>	44.6	9.9	10.1	47.8	27.3	26.2	49.1	31.4	29.9
<i>Crew</i>	45.2	9.1	9.1	46.6	24.5	22.8	47.7	20.1	20.0
<i>Harbor</i>	44.5	9.4	9.4	47.5	22.9	22.9	48.7	28.8	26.8
<i>Ice</i>	46.2	10.7	10.4	51.5	27.8	27.8	52.0	25.0	26.0
<i>Soccer</i>	45.1	10.0	10.2	47.7	18.4	18.0	49.2	26.7	24.1
Average	45.1	9.8	9.8	48.2	24.2	23.5	49.4	26.4	25.4

verify the proposed scheme has distorted the structural information present in the original video. Average SSIM value of video sequences without encryption is 0.993, while it is 0.164 and 0.180 for SE-CAVLC and SE-CABAC, respectively. Fig. 12 shows the framewise SSIM of *luma* of *Foreman* video sequence for I frames. It is important to note SSIM value of complex video sequences is less than that of simple video sequences.

2) *I+P Frames*: Video data normally consists of an I frame and a trail of P frames. I frames are inserted periodically to restrict the drift because of lossy compression and rounding errors. In these experiments, *intra period* is set at 10 in a sequence of 100 frames. Results shown in Table VIII verify the effectiveness of our scheme over the whole range of QP values for *Foreman* video sequence. Table IX verifies the performance of our algorithm for all video sequences for I+P frames at QP value 18. Average PSNR of *luma* for all the sequences is 9.75 dB and 10.02 dB for SE-CAVLC and SE-CABAC,

589 given in Table IV over whole QP range. It is also compared
590 with the PSNR obtained for the same video sequence without
591 encryption. In Table IV, we present PSNR of original video
592 only for CAVLC. PSNR for CABAC is very much similar as
593 presented in Table I. One can note that whatever is the QP
594 value, the quality of the encrypted video remains in the same
595 lower range.

596 Table V compares the average PSNR of 100 I frames
597 of all benchmark video sequences at QP value 18 without
598 encryption and with SE. Average PSNR value of *luma* for
599 all the sequences at QP value 18 is 9.49 dB for SE-CAVLC
600 and 9.80 dB for SE-CABAC. It confirms that this algorithm
601 works well for various combinations of motion, texture, and
602 objects for I frames. It is also evident in framewise PSNR
603 of *luma* of I frames of *Foreman* video sequence as shown in
604 Fig. 11. Table VI contains the experimental results of SE of
605 100 I frames for SD resolution. Here, average PSNR value of
606 *luma* is 9.82 dB for SE-CAVLC and 9.83 dB for SE-CABAC,
607 which is almost the same as that of QCIF resolution. It is
608 evident that this algorithm is capable to encrypt high-quality
609 information at all resolutions. For the rest of the section,
610 we present analysis for QCIF resolution only, since more
611 benchmark video sequences are available in this resolution.

612 Table VII shows the SSIM values of *luma* of benchmark
613 video sequences without encryption and with SE. Results

TABLE VII
SSIM COMPARISON OF *luma* OF I FRAMES WITHOUT ENCRYPTION AND WITH SE AT QP VALUE 18

Sequence	CAVLC	SE-CAVLC	CABAC	SE-CABAC
<i>Bus</i>	0.995	0.069	0.994	0.064
<i>City</i>	0.994	0.115	0.994	0.093
<i>Crew</i>	0.991	0.184	0.991	0.153
<i>Football</i>	0.991	0.219	0.991	0.184
<i>Foreman</i>	0.990	0.198	0.990	0.165
<i>Harbor</i>	0.998	0.047	0.998	0.038
<i>Ice</i>	0.990	0.419	0.990	0.398
<i>Mobile</i>	0.998	0.040	0.998	0.356
<i>Soccer</i>	0.988	0.185	0.988	0.171
Average	0.993	0.164	0.993	0.180

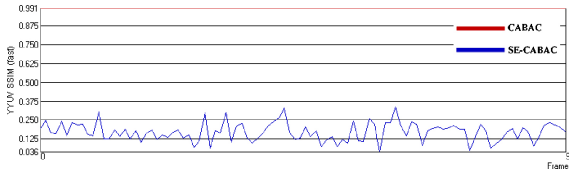


Fig. 12. Framewise SSIM of I frames for *Foreman* for SE-CABAC at QP value 18.

TABLE VIII
PSNR COMPARISON FOR I+P FRAMES WITHOUT ENCRYPTION AND WITH SE FOR *Foreman* AT DIFFERENT QP VALUES

Sequence	PSNR (Y) (dB)		PSNR (U) (dB)		PSNR (V) (dB)				
	ORIG	SE	ORIG	SE	ORIG	SE			
	CAVLC	CABAC	CAVLC	CABAC	CAVLC	CABAC			
12	49.6	8.7	8.1	49.9	18.4	23.0	50.6	10.4	21.6
18	43.9	9.1	10.4	45.5	23.6	23.9	47.6	8.0	23.2
24	38.9	9.6	9.7	42.0	26.9	24.9	44.3	25.8	25.0
30	34.6	9.2	9.2	39.8	28.6	24.9	41.5	26.6	24.0
36	30.7	10.1	8.2	37.9	28.4	24.3	38.8	22.8	23.3
42	27.0	9.4	8.6	36.3	26.5	26.8	36.9	25.6	24.6

632 respectively. Fig. 11 shows the framewise PSNR of *luma* of
 633 *Foreman* video sequence for I+P. Here, PSNR of SE-CAVLC
 634 and SE-CABAC remains almost the same for sequence of P
 635 frames and changes at every I frame, thus producing a staircase
 636 graph. SSIM quality metric has very low values and is not
 637 given here for the sake of brevity.

638 C. Security Analysis

639 1) Analysis of Entropy and Local Standard Deviation:

640 The security of the encrypted image can be measured by
 641 considering the variations (local or global) in the protected
 642 image. Entropy is a statistical measure of randomness or
 643 disorder of a system which is mostly used to characterize the
 644 texture in the input images. Considering this, the information
 645 content of image can be measured with the entropy $H(X)$ and
 646 local standard deviation $\sigma(j)$. If an image has 2^k gray levels
 647 α_i with $0 \leq i \leq 2^k$ and the probability of gray level α_i is
 648 $P(\alpha_i)$, and without considering the correlation of gray levels,
 649 the first order entropy $H(X)$ is defined as follows:

$$H(X) = - \sum_{i=0}^{2^k-1} P(\alpha_i) \log_2(P(\alpha_i)). \quad (4)$$

TABLE IX
COMPARISON OF PSNR WITHOUT ENCRYPTION AND WITH SE FOR I+P FRAMES AT QP VALUE 18

Sequence	PSNR (Y) (dB)		PSNR (U) (dB)		PSNR (V) (dB)				
	ORIG	SE	ORIG	SE	ORIG	SE			
	CAVLC	CABAC	CAVLC	CABAC	CAVLC	CABAC			
<i>Bus</i>	43.7	7.6	7.7	45.1	27.2	25.4	46.4	24.7	27.0
<i>City</i>	43.8	11.4	11.1	45.7	32.5	30.2	46.8	32.5	31.7
<i>Crew</i>	44.5	9.0	10.0	45.8	25.1	22.0	45.7	19.6	20.2
<i>Football</i>	44.2	12.1	11.3	45.7	14.3	14.6	46.1	24.8	24.3
<i>Foreman</i>	43.9	9.1	10.4	45.5	23.6	23.9	47.6	8.0	23.2
<i>Harbor</i>	43.7	9.5	9.8	45.4	24.5	22.9	46.6	33.9	31.7
<i>Ice</i>	46.1	10.9	10.4	48.6	23.6	25.3	49.1	19.2	19.7
<i>Mobile</i>	43.8	8.4	8.8	44.2	10.1	12.5	44.1	9.6	11.8
<i>Soccer</i>	43.6	9.6	10.6	46.5	21.8	20.8	47.8	27.4	22.2
Average	44.2	9.75	10.0	45.8	22.5	21.9	46.7	22.2	23.5

650 If the probability of each gray level in the image is
 651 $P(\alpha_i) = \frac{1}{2^k}$, then the encryption of such image is robust against
 652 statistical attacks of first order, and thus $H(X) = \log_2(2^k) =$
 653 k bits/pixel. In the image, the information redundancy r is
 654 defined as follows:

$$r = k - H(X). \quad (5)$$

655 Similarly, the local standard deviation $\sigma(j)$ for each pixel
 656 $p(j)$ taking account of its neighbors to calculate the local mean
 657 $\bar{p}(j)$, is given as follows:

$$\sigma(j) = \sqrt{\frac{1}{m} \sum_{i=1}^m (p(i) - \bar{p}(j))^2} \quad (6)$$

658 where m is the size of the pixel block to calculate the local
 659 mean and standard deviation, and $0 \leq j < M$, if M is
 660 the image size. In case of full encryption, entropy $H(X)$ is
 661 maximized with high values of local standard deviation. But
 662 in case of SE-CAVLC and SE-CABAC, the video frame is
 663 transformed to flat regions with blocking artifacts as depicted
 664 in Figs. 9 and 10. It is generally owing to variation in pixel
 665 values at MB boundaries. For all the benchmark sequences,
 666 the average information redundancy r for SE-CAVLC and SE-
 667 CABAC sequences is 0.94 and 0.55, respectively, while it is
 668 1.11 for all the original sequences. Despite the fact that SE-
 669 CAVLC and SE-CABAC transform the video frames into flat
 670 region, the entropy of the encrypted video sequences from
 671 (4) is higher as compared to the original sequences. These
 672 flat regions are because of two reasons. First, flat regions
 673 are due to the fact that prediction is performed from edge
 674 pixels of neighboring MBs. Second, pixels have either very
 675 high value (bright video frame) or very low value (dark video
 676 frame) in SE video frame. This is owing to the fact that during
 677 reconstruction pixel value are clipped to 255 if they are greater
 678 than it and to 0 if they are below this lower range. So if
 679 many pixels have value beyond the upper or lower range, all
 680 of them will be clipped to the same value, thus creating a flat
 681 region which is either dark or bright. Based on this analysis,
 682 the statistical characteristics of SE-CAVLC and SE-CABAC
 683 bitstreams vary from full encryption systems.

684 From (6), we also analyzed the local standard deviation
 685 σ for each pixel while taking into account its neighbors.

TABLE X
STANDARD DEVIATION FOR SE OF *Foreman* VIDEO SEQUENCE AT
DIFFERENT QP VALUES

QP	CAVLC		CABAC	
	ORIG	SE-CAVLC	ORIG	SE-CABAC
12	6.75	71.49	7.02	69.69
18	7.21	73.23	7.53	59.97
24	8.57	91.98	8.63	84.55
30	6.35	35.99	6.71	57.87
36	6.90	47.42	6.93	68.04
42	7.91	75.26	8.11	71.17



Fig. 13. Key sensitivity test for encrypted frame #1 of *Foreman* video sequence for QP value 18. Encrypted frames are decrypted and decoded with (a) original key, (b) 1-bit different key (SE-CAVLC), and (c) 1-bit different key (SE-CABAC).

686 In Table X, the mean local standard deviation for *Foreman*
687 sequence at different QP values is given. For all benchmark
688 video sequences, the mean local standard deviation of *luma*
689 equals to 69.15 and 61.48 for the SE-CAVLC and SE-CABAC
690 bitstreams, respectively, where the mean local standard deviation
691 is less than ten gray levels for the original benchmark
692 sequences. One can note that local standard deviation of
693 encrypted sequences is higher than original sequences.

694 2) *Correlation of Adjacent Pixels*: Visual data is highly
695 correlated, i.e., pixels values are highly probable to repeat in
696 horizontal, vertical, and diagonal directions. A correlation of a
697 pixel with its neighboring pixel is then given by a tuple (x_i, y_i)
698 where y_i is the adjacent pixel of x_i . Since there is always three
699 directions in images, i.e., horizontal, vertical, and diagonal, so
700 we can define correlation direction between any two adjacent
701 pixels as follows:

$$corr_{(x,y)} = \frac{1}{n-1} \sum_0^n \left(\frac{x_i - \bar{x}_i}{\sigma_x} \right) \left(\frac{y_i - \bar{y}_i}{\sigma_y} \right) \quad (7)$$

702 where n represents the total number of tuples (x_i, y_i) , \bar{x}_i and
703 \bar{y}_i represent the local mean, and σ_x and σ_y represent the local
704 standard deviation, respectively.

705 Owing to the flat regions in SE-CAVLC and SE-CABAC
706 video sequences, the correlation values in these sequences will
707 be higher as compared to original image which contain texture
708 and edges. For all the benchmark sequences, the average
709 horizontal correlation coefficient is 0.88 and 0.87 for the SE-
710 CAVLC and SE-CABAC, respectively, while it is 0.80 for the
711 original sequences.

712 3) *Key Sensitivity Test*: Robustness against cryptanalyst
713 can be improved if the cryptosystem is highly sensitive toward
714 the key. The more the visual data is sensitive toward the key,
715 the more we would have data randomness. For this purpose, a
716 key sensitivity test is assumed where we pick one key and then
717 apply the proposed technique for encryption and then make a
718 1 bit change in the key and decode the bitstream. Numerical
719 results show that the proposed technique is highly sensitive
720 toward the key change, i.e., a different version of encrypted
721 video sequence is produced when the keys are changed, as
722 shown in Fig. 13. PSNR of *luma* of decrypted frames with 1-
723 bit different key is 10.39 dB and 8.31 dB for SE-CAVLC and
724 SE-CABAC as shown in Table XI. It lies in the same lower
725 range as decoded frames without decryption.

726 4) *Removal of Encrypted Data Attack*: In another ex-
727 periment, we have replaced the encrypted bits with constant
728 values in order to measure the strength of SE-CAVLC and SE-

TABLE XI

KEY SENSITIVITY TEST OF SE-CAVLC AND SE-CABAC ENCRYPTED
VIDEO FOR FRAME #1 *Foreman* VIDEO SEQUENCE FOR QP VALUE 18

	PSNR (Y) (dB)	PSNR (U) (dB)	PSNR (V) (dB)
Original key	44.60	45.73	47.35
SE-CAVLC (1-bit different key)	10.39	24.46	14.02
SE-CABAC (1-bit different key)	8.31	25.13	24.82

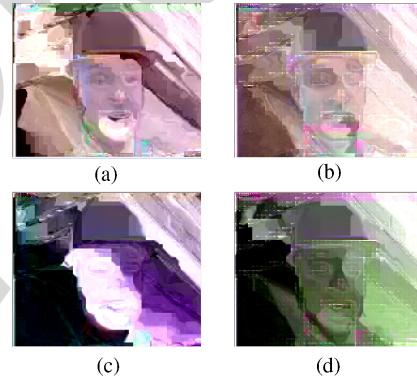


Fig. 14. Attack in the selectively encrypted image by removing the encrypted data. (a) SE-CAVLC encrypted image $\{Y, U, V\} = \{10.01, 26.86, 25.24\}$ dB. (b) SE-CAVLC attacked image $\{Y, U, V\} = \{8.87, 27.3, 26.3\}$ dB. (c) SE-CABAC encrypted image $\{Y, U, V\} = \{8.20, 17.95, 24.53\}$ dB. (d) SE-CABAC attacked image $\{Y, U, V\} = \{7.72, 28.6, 24.6\}$ dB.

729 CABAC proposed method as described in [27]. Here we have
730 used frame #1 of *Foreman* video sequence with QP value 24.
731 Fig. 14 shows both encrypted and attacked video frames for
732 SE-CAVLC and SE-CABAC. For example, Fig. 14(a) shows
733 SE-CAVLC video frame with PSNR = 10.01 dB for *luma*. If
734 we set the encrypted bits of all NZs to zero, we get the video
735 frame illustrated in Fig. 14(b) with *luma* PSNR = 8.87 dB.
736 Similarly, Fig. 14(c) shows SE-CABAC video frame having
737 PSNR = 8.20 dB while the attacked SE-CABAC video frame
738 has PSNR = 7.72 dB as shown in Fig. 14(d).

D. Comparative Evaluation

739 For the sake of comparative evaluation of our scheme, we
740 have compared it with six other recent techniques, which
741 include scrambling [9], NAL unit encryption [14], MB header
742 encryption [16], reversible ROI encryption [5], I frame en-
743 cryption [2], and multiple Huffman table permutation [36].
744 These techniques are different from each other in several
745

TABLE XII
COMPARISON OF PROPOSED SCHEME WITH OTHER RECENT METHODS

Video SE Scheme	Format Compliant	Robust to Transcoding	Domain	Bitrate Increase	Compression Independent	Encryption Algorithm
Scrambling for privacy protection [9]	Yes	No	Transform	Yes	Yes	Pseudo random sign inversion
NAL unit encryption [14]	No	No	Bitstream	No	No	Stream cipher
MB header data encryption [16]	No	No	Transform	No	No	Stream cipher
Reversible encryption of ROI [5]	Yes	Yes	Pixel	Yes	Yes	Pseudo random pixel permutations
I frame encryption [2]	No	No	Bitstream	No	No	AES
Multiple Huffman tables [36]	No	No	Bitstream	Yes	No	Huffman table permutations
Our scheme	Yes	No	Bitstream ^a	No	No	AES (CFB mode)

^aFor SE-CAVLC, bitstream is encrypted, while for SE-CABAC, binstrings are encrypted as explained in Section III-B.

746 aspects, e.g., working domain (pixel, transform, or bitstream)
 747 and encryption algorithm (pseudo random permutation, stream
 748 cipher, or AES). The comparison has been made based on
 749 several important characteristics of SE systems and is summa-
 750 rized in Table XII. Encryption algorithm used in SE scheme
 751 is of vital importance for the security level. AES has the
 752 highest security among all the known ciphers and our proposed
 753 scheme utilizes AES. Among the recent techniques, AES has
 754 been used only in [2] but their SE scheme is very naive and
 755 encrypts only I frames.

756 SE should not result in increase of bitrate. For example, if
 757 a video for 3G wireless connection has bitrate of 384 kb/s, its
 758 encrypted version should have the same bitrate. Otherwise, it
 759 cannot be played back on 3G connection. Our scheme keeps
 760 the bitrate intact. It is in contrast to other schemes which either
 761 allow increase in bitrate [5], [9], [36] or use stream cipher
 762 for the sake of same bitrate [14], [16], thus compromising on
 763 the security of the system.

764 Format compliance is another important aspect for en-
 765 crypted video data. Most of the schemes are not format
 766 complaint and their encrypted bitstreams cannot be decoded
 767 by reference decoder except SE schemes which work in pixel
 768 domain [5] and transform domain [9].

769 Our SE-CABAC scheme is the first format compliant tech-
 770 nique which is for arithmetic coding-based entropy coding
 771 module, while keeping the bitrate unchanged. Recent encryp-
 772 tion techniques for arithmetic coding [11], [13] are not format
 773 complaint and require lot of processing power.

774 To summarize, our proposed schemes (SE-CAVLC and
 775 SE-CABAC) meet all the requirements of an integrated
 776 compression-encryption system. Our proposed system is fully
 777 compliant to H.264/AVC decoder, with no change in bitrate
 778 and has the security of AES cipher.

779 V. CONCLUSION

780 In this paper, an efficient SE system has been proposed for
 781 H.264/AVC video codec for CAVLC and CABAC. The SE
 782 is performed in the entropy coding stage of the H.264/AVC
 783 using the AES encryption algorithm in the CFB mode. In
 784 this way, the proposed encryption method does not affect
 785 the bitrate and the H.264/AVC bitstream compliance. The SE
 786 is performed in CAVLC codewords and CABAC binstrings
 787 such that they remain a valid codewords/binstrings thereafter
 788 having exactly the same length. Experimental analysis has

789 been presented for I and P frames. The proposed scheme
 790 can be used for B frames without any modification, since B
 791 frames are also inter-frames but have bidirectional prediction.
 792 The proposed method has the advantage of being suitable for
 793 streaming over heterogeneous networks because of no change
 794 in bitrate. The experiments have shown that we can achieve
 795 the desired level of encryption, while maintaining the full
 796 bitstream compliance, under a minimal set of computational
 797 requirements. The presented security analysis confirmed a
 798 sufficient security level for multimedia applications in the
 799 context of SE. The proposed system can be extended for ROI-
 800 specific video protection [26] for video surveillance and can
 801 be applied to medical video transmission [24].

802 REFERENCES

803 [1] *Draft ITU-T Recommendation and Final Draft International Standard of*
 804 *Joint Video Specification (ITU-T Rec. H.264/ISO/IEC 14496-10 AVC)*,
 805 document JVT-G050, Joint Video Team (JVT), Mar. 2003.
 806 [2] M. Abomhara, O. Zakaria, O. Khalifa, A. Zaiden, and B. Zaiden, "En-
 807 hancing selective encryption for H.264/AVC using advanced encryption
 808 standard," *Int. J. Comput. Electric. Eng.*, vol. 2, no. 2, pp. 223–229,
 809 2010.
 810 [3] M. Bellare, T. Ristenpart, P. Rogaway, and T. Stegers, "Format-
 811 preserving encryption," in *Proc. 16th Annu. Int. Workshop Selected*
 812 *Areas Cryptography*, 2009, pp. 295–312.
 813 [4] G. Bjontegaard and K. Lillevold, *Context-Adaptive VLC Coding of*
 814 *Coefficients*, document JVT-C028, Joint Video Team, Fairfax, VA, May
 815 2002.
 816 [5] P. Carrillo, H. Kalva, and S. Magliveras, "Compression independent
 817 reversible encryption for privacy in video surveillance," *EURASIP J.*
 818 *Inform. Security*, vol. 2009, p. 13, 2009.
 819 [6] H. Cheng and X. Li, "Partial encryption of compressed images and
 820 videos," *IEEE Trans. Signal Process.*, vol. 48, no. 8, pp. 2439–2445,
 821 Aug. 2000.
 822 [7] J. Daemen and V. Rijmen, "AES proposal: The Rijndael clock cipher,"
 823 Proton World Int., Katholieke Univ. Leuven, ESAT-COSIC, Leuven,
 824 Belgium, Tech. Rep., 2002.
 825 [8] M. V. Droogenbroeck and R. Benedett, "Techniques for a selective
 826 encryption of uncompressed and compressed images," in *Proc. ACIVS*,
 827 Sep. 2002, pp. 90–97.
 828 [9] F. Dufaux and T. Ebrahimi, "Scrambling for privacy protection in video
 829 surveillance systems," *IEEE Trans. Circuits Syst. Video Technol.*, vol. 18,
 830 no. 8, pp. 1168–1174, Aug. 2008.
 831 [10] M. M. Fisch, H. Stgner, and A. Uhl, "Layered encryption techniques
 832 for DCT-coded visual data," in *Proc. 12th EUSIPCO*, Sep. 2004, pp.
 833 821–824.
 834 [11] M. Grangotto, E. Magli, and G. Olmo, "Multimedia selective encryption
 835 by means of randomized arithmetic coding," *IEEE Trans. Multimedia*,
 836 vol. 8, no. 5, pp. 905–917, Oct. 2006.
 837 [12] G. Jakimoski and K. Subbalakshmi, "Cryptanalysis of some multimedia
 838 encryption schemes," *IEEE Trans. Multimedia*, vol. 10, no. 3, pp.
 839 330–338, Apr. 2008.

- [13] W. Jiangtao, K. Hyungjin, and J. Villasenor, "Binary arithmetic coding with key-based interval splitting," *IEEE Signal Process. Lett.*, vol. 13, no. 2, pp. 69–72, Feb. 2006.
- [14] C. Li, X. Zhou, and Y. Zong, "NAL level encryption for scalable video coding," in *Proc. PCM*, no. 5353. 2008, pp. 496–505.
- [15] S. Lian, Z. Liu, Z. Ren, and Z. Wang, "Selective video encryption based on advanced video coding," in *Proc. PCM*, no. 3768. 2005, pp. 281–290.
- [16] S. Lian, Z. Liu, Z. Ren, and H. Wang, "Commutative encryption and watermarking in video compression," *IEEE Trans. Circuits Syst. Video Technol.*, vol. 17, no. 6, pp. 774–778, Jun. 2007.
- [17] E. Lin, A. Eskicioglu, R. Lagendijk, and E. Delp, "Advances in digital video content protection," *Proc. IEEE*, vol. 93, no. 1, pp. 171–183, Jan. 2005.
- [18] T. Lookabaugh and D. Sicker, "Selective encryption for consumer applications," *IEEE Commun. Mag.*, vol. 42, no. 5, pp. 124–129, May 2004.
- [19] R. Lukac and K. Plataniotis, "Bit-level based secret sharing for image encryption," *Patt. Recog.*, vol. 38, no. 5, pp. 767–772, May 2005.
- [20] D. Marpe, H. Schwarz, and T. Wiegand, "Context-based adaptive binary arithmetic coding in the H.264/AVC video compression standard," *IEEE Trans. Circuits Syst. Video Technol.*, vol. 13, no. 7, pp. 620–636, Jul. 2003.
- [21] K. Martin, R. Lukac, and K. Plataniotis, "Efficient encryption of wavelet-based coded color images," *Patt. Recog.*, vol. 38, no. 7, pp. 1111–1115, Jul. 2005.
- [22] I. Moccagatta and K. Ratakonda, *A Performance Comparison of CABAC and VCL-Based Entropy Coders for SD and HD Sequences*, document JVT-E079r2, Joint Video Team (JVT), Oct. 2002.
- [23] S. Ou, H. Chung, and W. Sung, "Improving the compression and encryption of images using FPGA-based cryptosystems," *Multimedia Tools Applicat.*, vol. 28, no. 1, pp. 5–22, Jan. 2006.
- [24] W. Puech and J. Rodrigues, "A new crypto-watermarking method for medical images safe transfer," in *Proc. 12th EUSIPCO*, 2004, pp. 1481–1484.
- [25] J.-M. Rodrigues, W. Puech, and A. Bors, "A selective encryption for heterogeneous color JPEG images based on VLC and AES stream cipher," in *Proc. Eur. Conf. CGIV*, Jun. 2006, pp. 34–39.
- [26] J.-M. Rodrigues, W. Puech, and A. Bors, "Selective encryption of human skin in JPEG images," in *Proc. IEEE Int. Conf. Image Process.*, Oct. 2006, pp. 1981–1984.
- [27] A. Said, "Measuring the strength of partial encryption scheme," in *Proc. IEEE Int. Conf. Image Process.*, vol. 2, Sep. 2005, pp. 1126–1129.
- [28] B. Schneier, *Applied Cryptography*. New York: Wiley, 1995.
- [29] Z. Shahid, M. Chaumont, and W. Puech, "Fast protection of H.264/AVC by selective encryption," in *Proc. SinFra IPAL Symp.*, Feb. 2009, pp. 11–21.
- [30] Z. Shahid, M. Chaumont, and W. Puech, "Fast protection of H.264/AVC by selective encryption of CABAC for I&P frames," in *Proc. 17th EUSIPCO*, Aug. 2009, pp. 2201–2205.
- [31] D. R. Stinson, *Cryptography: Theory and Practice (Discrete Mathematics and Its Applications)*. New York: Chapman and Hall/CRC Press, Nov. 2005.
- [32] L. Tang, "Methods for encrypting and decrypting MPEG video data efficiently," in *Proc. ACM Multimedia*, vol. 3, 1996, pp. 219–229.
- [33] Z. Wang, A. Bovik, H. Sheikh, and E. Simoncelli, "Image quality assessment: From error visibility to structural similarity," *IEEE Trans. Image Process.*, vol. 13, no. 4, pp. 600–612, Apr. 2004.
- [34] J. Wen, M. Severa, W. Zeng, M. Luttrell, and W. Jin, "A format-compliant configurable encryption framework for access control of video," *IEEE Trans. Circuits Syst. Video Technol.*, vol. 12, no. 6, pp. 545–557, Jun. 2002.
- [35] T. Wiegand, G. J. Sullivan, G. Bjontegaard, and A. Luthra, "Overview of the H.264/AVC video coding standard," *IEEE Trans. Circuits Syst. Video Technol.*, vol. 13, no. 7, pp. 560–576, Jul. 2003.
- [36] C.-P. Wu and C.-C. Kuo, "Design of integrated multimedia compression and encryption systems," *IEEE Trans. Multimedia*, vol. 7, no. 5, pp. 828–839, Oct. 2005.
- [37] K. Yabuta, H. Kitazawa, and T. Tanaka, "A new concept of security camera monitoring with privacy protection by masking moving objects," in *Proc. Adv. Multimedia Inform. Process.*, vol. 1, no. 3767. 2005, pp. 831–842.
- [38] W. Zeng and S. Lei, "Efficient frequency domain selective scrambling of digital video," *IEEE Trans. Multimedia*, vol. 5, no. 1, pp. 118–129, Mar. 2003.
- [39] S. Ziauddin, I. U. Haq, and M. A. Khan, "Method and system for fast context based adaptive binary arithmetic coding," U.S. Patent 7 221 296, 2007.



Zafar Shahid received the B.S. degree in electrical engineering from the University of Engineering and Technology, Lahore, Pakistan, and the M.S. degree in image processing from the National Institute of Applied Sciences, Lyon, France, in 2001 and 2007, respectively. Currently, he is a Ph.D. student at the Laboratory of Computer Science, Robotics, and Microelectronics, University of Montpellier II, Montpellier, France.

Before his M.S. degree, he was a Senior Embedded System Engineer with Streaming Networks, Santa Clara, CA, where he was involved in the research and development in the domain of video processing. His current research interests include compression, watermarking, and encryption of scalable video.



Marc Chaumont was born in November 1976, in France. He received the Engineering Diploma degree from the National Institute of Applied Sciences (INSA), Rennes, France, in 1999, and the Ph.D. degree from the IRISA Rennes (INRIA, CNRS, University of Rennes 2, and INSA) in 2003, both in computer sciences.

His Ph.D. thesis was about video objects representations, with dynamic coding and scalability functionalities, in the video compression area. He has carried on research activities for one year at the

INRIA Rennes and for another year at the University Technological Institute, Bayonne, France, as a Visiting Assistant Professor. During this last year, he focused on face tracking using a deformable 3-D face model. Since September 2005, he is an Assistant Professor with the Laboratory of Computer Science, Robotics, and Microelectronics, Montpellier, France, and the University of Nîmes, Nîmes, France. His current research interests include watermarking, steganography, video compression, and to a lesser extent segmentation and tracking in videos.



William Puech (M'XX) received the Diploma degree in electrical engineering from the University of Montpellier, Montpellier, France, in 1991, and the Ph.D. degree in signal-image-speech from the Polytechnic National Institute, Grenoble, France, in 1997.

He started his research activities in image processing and computer vision. He was a Visiting Research Associate with the University of Thessaloniki, Thessaloniki, Greece. From 1997 to 2000, he was an Assistant Professor with the University of Toulon, Toulon, France, with research interests including methods of active contours applied to medical images sequences. Between 2000 and 2008, he was an Associate Professor and since 2009, he has been a Full Professor of image processing with the Laboratory of Computer Science, Robotics, and Microelectronics, University of Montpellier. He has developed applications on medical images, cultural heritage, and video surveillance. He is the Head of the ICAR Team (Image and Interaction), University of Montpellier. He has published more than 12 journal papers, 4 book chapters, and more than 65 conference papers. His current research interests include the areas of protection of visual data (image, video, and 3-D object) for safe transfer by combining watermarking, data hiding, compression, and cryptography.

Prof. Puech is a reviewer for more than 15 journals (IEEE TRANSACTIONS ON IMAGE PROCESSING, IEEE TRANSACTIONS ON MULTIMEDIA, *Signal Processing: Image Communication*, *Journal of Applied Signal Processing*, *Journal of Electronic Imaging*, and others) and more than ten conference proceedings (IEEE ICIP, EUSIPCO, WIAMIS, IWDW, and others). He is currently a member of SPIE. Since 2005, he has been in the Technical Program Committee of EUSIPCO, and since 2009, he has been in the Area Chair "Image and Multidimensional Signal Processing" of EUSIPCO.

914
915
916
917
918
919
920
921
922
923
924
925
926
927
928
929
930
931
932
933
934
935
936
937
938
939
940
941
942
943
944
945
946
947
948
949
950
951
952
953
954
955
956
957
958
959
960
961
962
963
964
965
966
967
968
969
970
971
972
973
974
975
976
977
978
979

AQ:7

AQ:8

AUTHOR QUERIES

AUTHOR PLEASE ANSWER ALL QUERIES

- 980
981 AQ:1= Please provide the expanded form of NZs.
982 AQ:2= Please provide the expanded form of AC and DC.
983 AQ:3= Please provide the expanded form of SD.
984 AQ:4= Please verify the volume no. in Ref. [5].
985 AQ:5= Please provide the issue no. or month in Ref. [5].
986 AQ:6= Please provide the technical report no. in Ref. [7].
987 AQ:7= Please provide the membership year of Puech.
988 AQ:8= Please verify the sense of the sentence "...he has been in the Area Chair..."
- 989 END OF ALL QUERIES

IEEE PROOF

Fast Protection of H.264/AVC by Selective Encryption of CAVLC and CABAC for I and P Frames

Zafar Shahid, Marc Chaumont, and William Puech, *Member, IEEE*

Abstract—This paper presents a novel method for the protection of bitstreams of state-of-the-art video codec H.264/AVC. The problem of selective encryption (SE) is addressed along with the compression in the entropy coding modules. H.264/AVC supports two types of entropy coding modules. Context-adaptive variable length coding (CAVLC) is supported in H.264/AVC baseline profile and context-adaptive binary arithmetic coding (CABAC) is supported in H.264/AVC main profile. SE is performed in both types of entropy coding modules of this video codec. For this purpose, in this paper the encryption step is done simultaneously with the entropy coding CAVLC or CABAC. SE is performed by using the advanced encryption standard (AES) algorithm with the cipher feedback mode on a subset of codewords/binstrings. For CAVLC, SE is performed on equal length codewords from a specific variable length coding table. In case of CABAC, it is done on equal length binstrings. In our scheme, entropy coding module serves the purpose of encryption cipher without affecting the coding efficiency of H.264/AVC by keeping exactly the same bitrate, generating completely compliant bitstream and utilizing negligible computational power. Owing to no escalation in bitrate, our encryption algorithm is better suited for real-time multimedia streaming over heterogeneous networks. It is perfect for playback on handheld devices because of negligible increase in processing power. Nine different benchmark video sequences containing different combinations of motion, texture, and objects are used for experimental evaluation of the proposed algorithm.

Index Terms—AES algorithm, CABAC, CAVLC, selective encryption, stream cipher, video security.

I. INTRODUCTION

WITH THE RAPID growth of processing power and network bandwidth, many multimedia applications have emerged in the recent past. As digital data can easily be copied and modified, the concern about its protection and authentication have surfaced. Digital rights management (DRM) has emerged as an important research field to protect the copyrighted multimedia data. DRM systems enforce the rights

Manuscript received December 9, 2009; revised May 18, 2010; accepted July 6, 2010. This work is supported in part by the VOODOO Project (2008–2011), which is a French national project of Agence Nationale de la Recherche (ANR), and the region of Languedoc Roussillon, France. This paper was recommended by Associate Editor M. Barni.

The authors are with the Laboratory of Informatics, Robotics, and Microelectronics, University of Montpellier II, Montpellier 34392, France (e-mail: zafar.shahid@lirmm.fr; marc.chaumont@lirmm.fr; william.puech@lirmm.fr).

Color versions of one or more of the figures in this paper are available online at <http://ieeexplore.ieee.org>.

Digital Object Identifier 10.1109/TCSVT.2011.2129090

of the multimedia property owners while ensuring the efficient rightful usage of such property.

Multimedia data requires either full encryption or selective encryption (SE) depending on the application requirements. For example, military and law enforcement applications require full encryption. Nevertheless, there is a large spectrum of applications that demands security on a lower level, as, e.g., that ensured by SE. SE encrypts part of the plaintext and has two main advantages. First, it reduces the computational requirements, since only a part of plaintext is encrypted [6]. Second, encrypted bitstream maintains the essential properties of the original bitstream [3]. SE just prevents abuse of the data. In the context of video, it refers to destroying the commercial value of video to a degree which prevents a pleasant viewing experience.

SE schemes based on H.264/AVC have been already presented on context-adaptive variable length coding (CAVLC) [29] and context-adaptive binary arithmetic coding (CABAC) [30]. These two previous methods fulfill real-time constraints by keeping the same bitrate and by generating completely compliant bitstream. In this paper, we have enhanced the previous proposed approaches by encryption of more syntax elements for CAVLC and extending it for P frames. Here, we have also used advanced encryption standard (AES) [7] in the cipher feedback (CFB) mode which is a stream cipher algorithm. Security of the proposed schemes has also been analyzed in detail.

The rest of this paper is organized as follows. In Section II, overview of H.264/AVC and AES algorithm is presented. We explain the whole system architecture of the proposed methods in Section III. Section IV contains experimental evaluation and security analysis. In Section V, we present the concluding remarks about the proposed schemes.

II. DESCRIPTION OF THE H.264/AVC-BASED VIDEO ENCRYPTION SYSTEM

A. Overview of H.264/AVC

H.264/AVC (also known as MPEG4 Part 10) [1] is state-of-the-art video coding standard of ITU-T and ISO/IEC. H.264/AVC has some additional features and outperforms previous video coding standards including MPEG2 and MPEG4 Part II [35]. We review the basic working of CAVLC in Section II-A1 and of CABAC in Section II-A2.

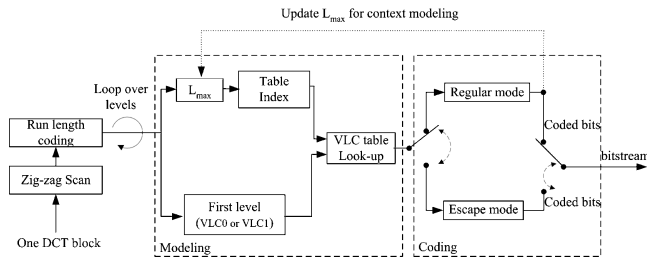


Fig. 1. Block diagram of level coding in CAVLC of H.264/AVC.

1) *CAVLC*: In CAVLC, run-length coding is performed first as it encodes levels and runs separately. CAVLC is designed to exploit the characteristics of NZs and works in several steps.

To adapt to the local statistical features of discrete cosine transform (DCT) coefficients, CAVLC uses seven fixed variable length coding (VLC) tables. For example, “2” will be coded as “010” using VLC1 table, while it will be coded as “1010” using VLC3 table. If magnitude of NZ lies within the range of that VLC table, it is coded by regular mode, otherwise escape mode is used. Adaptive nature is introduced by changing the table for the next NZ based on the magnitude of the current NZ as shown in Fig. 1. For the first NZ, VLC0 table is used unless there are more than ten NZs and less than three trailing ones, in which case it is coded with VLC1 table.

2) *CABAC*: CABAC is designed to better exploit the characteristics of NZs as compared to CAVLC, consumes more processing, and offers about 10% better compression than CAVLC on average [22]. Run-length coding has been replaced by significant map coding which specifies the position of NZs in the 4×4 block. Binary arithmetic coding (BAC) module of CABAC uses many context models to encode NZs and context model for a specific NZ depends on recently coded NZs.

CABAC consists of multiple stages as shown in Fig. 2(a). First of all, binarization is done in which non-binary syntax elements are converted to binary form called binstrings which are more amenable to compression by BAC. Binary representation for a non-binary syntax element is done in such a way that it is close to minimum redundancy code. In CABAC, there are four basic code trees for binarization step, namely, the *unary* code, the *truncated unary* code, the *kth order Exp-Golomb* code (EGk), and the *fixed length* code as shown in Fig. 2(b).

For an unsigned integer value $x \geq 0$, the unary code consists of x 1s plus a terminating 0 bit. The truncated unary code is only defined for x with $0 \leq x \leq s$. For $x < s$, the code is given by the unary code, whereas for $x = s$ the terminating “0” bit is neglected. EGk is constructed by a concatenation of a prefix and a suffix parts and is suitable for binarization of syntax elements that represent prediction residuals. For a given unsigned integer value $x > 0$, the prefix part of the EGk binstring consists of a unary code corresponding to the length $l(x) = \lceil \log_2(\frac{x}{2k} + 1) \rceil$. The EGk suffix part is computed as the binary representation of $x + 2^k(1 - 2^{l(x)})$ using $k + l(x)$ significant bits. Consequently for EGk binarization, the code length is $2l(x) + k + 1$. When $k = 0$, $2l(x) + k + 1 = 2l(x) + 1$.

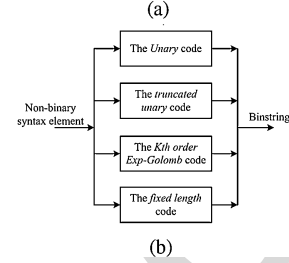
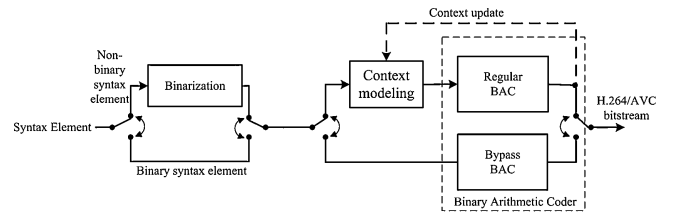


Fig. 2. (a) Block diagram of CABAC of H.264/AVC. (b) Binarization stage.

The fixed length code is applied to syntax elements with a nearly uniform distribution or to syntax elements, for which each bit in the fixed length code binstring represents a specific coding decision, e.g., coded block flag. Three syntax elements are binarized by concatenation of the basic code trees, namely, coded block pattern, NZ, and the motion vector difference (MVD). Binarization of absolute level of NZs is done by concatenation of truncated unary code and EG0. The truncated unary code constitutes the prefix part with cutoff value $S = 14$. Binarization and subsequent arithmetic coding process is applied to the syntax element $coeff_abs_value_minus1 = abs_level - 1$, since quantized transformed coefficients with zero magnitude are encoded using significant map. For MVD, binstring is constructed by concatenation of the truncated unary code and EG3. The truncated unary constitutes the prefix part with cutoff value $S = 9$. Suffix part of MVDs contains EG3 of $|MVD| - 9$ for $|MVD| > 9$ and sign bit.

B. AES Encryption Algorithm

The AES algorithm consists of a set of processing steps repeated for a number of iterations called rounds [7]. The number of rounds depends on the size of the key and the size of the data block. The number of rounds is nine, e.g., if both the block and the key are 128 bits long. Given a sequence $\{X_1, X_2, \dots, X_n\}$ of bit plaintext blocks, each X_i is encrypted with the same secret key k producing the ciphertext blocks $\{Y_1, Y_2, \dots, Y_n\}$. To encipher a data block X_i in AES, you first perform an AddRoundKey step by XORing a subkey with the block. The incoming data and the key are added together in the first AddRoundKey step. Afterward, it follows the round operation. Each regular round operation involves four steps which are SubBytes, ShiftRows, MixColumns, and AddRoundKey. Before producing the final ciphered data Y_i , the AES performs an extra final routine that is composed of SubBytes, ShiftRows, and AddRoundKey steps.

The AES algorithm can support several cipher modes: electronic code book (ECB), cipher block chaining, output feedback (OFB), CFB, and counter (CTR) [31]. The ECB mode is actually the basic AES algorithm. In CFB mode, as

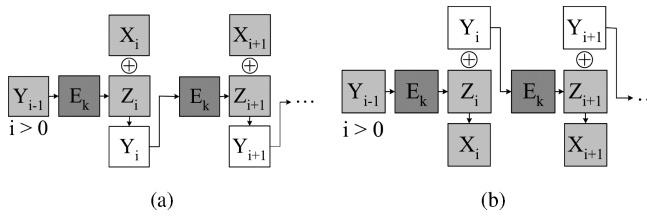


Fig. 3. CFB stream cipher. (a) Encryption. (b) Decryption.

163 shown in Fig. 3, the keystream element Z_i is generated and
 164 the ciphertext block Y_i is produced as follows:

$$\begin{cases} Z_i = E_k(Y_{i-1}), \text{ for } i \geq 1 \\ Y_i = X_i \oplus Z_i \end{cases} \quad (1)$$

165 where \oplus is the XOR operator.

166 Although AES is a block cipher, in the OFB, CFB, and
 167 CTR modes it operates as a stream cipher.

168 C. SE of Image and Video

169 SE is a technique aiming to save computational time or to
 170 enable new system functionalities by only encrypting a portion
 171 of a compressed bitstream while still achieving adequate
 172 security [18]. SE as well as partial encryption (PE) are applied
 173 only on certain parts of the bitstream. In the decoding stage,
 174 both the encrypted and the non-encrypted information should
 175 be appropriately identified and displayed [6], [21], [26]. The
 176 copyright protection of the multimedia content is a required
 177 feature for DRM systems. The technical challenges posed
 178 by such systems are high and previous approaches have not
 179 entirely succeeded in tackling them [17].

180 In [32], Tang proposed a technique called zigzag permutation
 181 applicable to DCT-based image and video codecs. On one
 182 hand, this method provides a certain level of confidentiality,
 183 while on the other hand, it increases the overall bitrate.
 184 For image, several SE techniques have been proposed in
 185 the literature. In [8], Droogenbroeck and Benedett proposed
 186 a technique for encryption of JPEG images. It encrypts a
 187 selected number of AC coefficients. The DC coefficients are
 188 not ciphered since they carry important visual information
 189 and they are highly predictable. In spite of the constancy
 190 in the bitrate while preserving the bitstream compliance, the
 191 compression and the encryption process are separated and
 192 consequently the computational complexity is increased.

193 The AES [7] has been used for SE of image and video in
 194 the literature. The AES was applied on the Haar discrete
 195 wavelet transform compressed images in [23]. The encryption
 196 of color images in the wavelet transform has been addressed
 197 in [21]. In this approach, the encryption is performed on the
 198 resulting wavelet code bits. In [25], SE was performed on color
 199 JPEG images by selectively encrypting only *luma* component
 200 using AES cipher. The protection rights of individuals and the
 201 privacy of certain moving objects in the context of security
 202 surveillance systems using viewer generated masking and the
 203 AES encryption standard has been addressed in [37].

204 Combining PE and image/video compression using the set
 205 partitioning in hierarchical trees was used in [6]. Nevertheless,
 206 this approach requires a significant computational complexity.

207 A method that does not require significant processing time and
 208 which operates directly on the bit planes of the image was
 209 proposed in [19]. The robustness of partially encrypted videos
 210 to attacks which exploit the information from non-encrypted
 211 bits together with the availability of side information was
 212 studied in [27]. Fisch *et al.* [10] proposed a scalable encryption
 213 method for a DCT-coded visual data wherein the data are
 214 organized in a scalable bitstream form. These bitstreams are
 215 constructed with the DC and some AC coefficients of each
 216 block which are then arranged in layers according to their
 217 visual importance, and PE process is applied over these layers.

218 For video, there are several SE techniques for different
 219 video codecs presented in the literature. SE of MPEG4 video
 220 standard was studied in [34] wherein data encryption standard
 221 was used to encrypt fixed length and variable length codes. In
 222 this approach, the encrypted bitstream is completely compliant
 223 with MPEG4 bitstream format but it increases the bitrate.
 224 A tradeoff has to be made among complexity, security, and
 225 the bit overhead. In [38], SE of MPEG4 video standard is
 226 proposed by doing frequency domain selective scrambling,
 227 DCT block shuffling, and rotation. This scheme is very easy to
 228 perform but its limitation is its bitrate overhead. SE of region
 229 of interest (ROI) of MPEG4 video has been presented in [9].
 230 It performs SE by pseudo randomly inverting sign of DCT
 231 coefficients in ROI. SE of H.264/AVC has been studied in [15]
 232 wherein encryption has been carried out in some fields like
 233 intra-prediction mode, residual data, inter-prediction mode,
 234 and motion vectors. A scheme for commutative encryption
 235 and watermarking of H.264/AVC is presented in [16]. Here,
 236 SE of some macroblock (MB) header fields is combined
 237 with watermarking of magnitude of DCT coefficients. This
 238 scheme presents a watermarking solution in encrypted domain
 239 without exposing video content. The limitation of techniques
 240 proposed in [15] and [16] is that they are not format compliant.
 241 Encryption for H.264/AVC has been discussed in [5] wherein
 242 they do permutations of the pixels of MBs which are in ROI.
 243 The drawback of this scheme is that bitrate increases as the
 244 size of the ROI increases. This is due to change in the statistics
 245 of ROI as it is no more a slow varying region which is
 246 the basic assumption for video signals. SE of H.264/AVC at
 247 network abstraction layer (NAL) has been proposed in [14].
 248 Important NAL units, namely, instantaneous decoding refresh
 249 picture, sequence parameter set, and picture parameter set are
 250 encrypted with a stream cipher. The limitation of this scheme
 251 is that it is not format compliant and cannot be parsed even at
 252 frame level. SE of H.264/AVC using AES has been proposed
 253 in [2]. In this scheme, encryption of I frame is performed,
 254 since P and B frame are not significant without I frames. This
 255 scheme is not format compliant.

256 The use of general entropy coder as encryption cipher
 257 using statistical models has been studied in the literature
 258 in [36]. It encrypts by using different Huffman tables for
 259 different input symbols. The tables, as well as the order
 260 in which they are used, are kept secret. This technique is
 261 vulnerable to known plaintext attacks as explained in [12].
 262 Key-based interval splitting of arithmetic coding (KSAC) has
 263 used an approach [13] wherein intervals are partitioned in each
 264 iteration of arithmetic coding. Secret key is used to decide

265 how the interval will be partitioned. Number of subintervals in
 266 which an interval is divided should be kept small as it increases
 267 the bitrate of bitstream. Randomized arithmetic coding [11]
 268 is aimed at arithmetic coding but instead of partitioning of
 269 intervals like in KSAC, secret key is used to scramble the
 270 order of intervals. The limitation of these entropy coding-based
 271 techniques is that encrypted bitstream is not format compliant.
 272 Moreover, these techniques require lot of processing power.

273 In the context of DRM systems, our paper addresses
 274 the simultaneous SE and compression for state-of-the-art
 275 H.264/AVC. The encrypted bitstream is format compliant with
 276 absolutely no escalation in bitrate. Furthermore, it does not
 277 require lot of processing power for encryption and decryption.
 278 In Section III, we describe our proposed approaches to
 279 apply SE and H.264/AVC compression in video sequences,
 280 simultaneously.

281 III. PROPOSED SE SCHEMES

282 Our approach consists of SE during the entropy coding
 283 stage of H.264/AVC. In baseline profile, SE is performed in
 284 CAVLC entropy coding stage (SE-CAVLC). While in main
 285 profile, it is performed in CABAC entropy coding stage (SE-
 286 CABAC). In SE of video, encrypted bitstream compliance is a
 287 required feature for some direct operations such as displaying,
 288 time seeking, and browsing. Encrypted bitstream will be
 289 compliant and fulfills real-time constraints if the following
 290 three conditions are fulfilled.

- 291 1) To keep the bitrate of encrypted bitstream same as the
- 292 original bitstream, encrypted codewords/binstrings must
- 293 have the same size as the original codewords/binstrings.
- 294 2) The encrypted codewords/binstrings must be valid so
- 295 that they may be decoded by entropy decoder.
- 296 3) The decoded value of syntax element from encrypted
- 297 codewords/binstrings must stay in the valid range for
- 298 that syntax element. Any syntax element which is used
- 299 for prediction of neighboring MBs should not be encr-
- 300 ypted. Otherwise, the drift in the value of syntax ele-
- 301 ment will keep on increasing and after a few iterations,
- 302 value of syntax element will fall outside the valid range
- 303 and bitstream will be no more decodable.

304 In each MB, header information is encoded first, which is
 305 followed by the encoding of MB data. To keep the bitstream
 306 compliant, we cannot encrypt MB header, since it is used
 307 for prediction of future MBs. MB data contains NZs and
 308 can be encrypted. A MB is further divided into 16 blocks of
 309 4×4 pixels to be processed by integer transform module. The
 310 coded block pattern is a syntax element used to indicate which
 311 8×8 blocks within a MB contain NZs. The *macroblock mode*
 312 (MBmode) is used to indicate whether a MB is *skipped* or not.
 313 If MB is not *skipped*, then MBmode indicates the prediction
 314 method for a specific MB. For a 4×4 block inside MB, if
 315 coded block pattern and MBmode are set, it indicates that this
 316 block is encoded. Inside 4×4 block, coded block flag is the
 317 syntax element used to indicate whether it contains NZs or not.
 318 It is encoded first. If it is zero, no further data is transmitted;
 319 otherwise, it is followed by encoding of significant map in
 320 case of CABAC. Finally, the absolute value of each NZ and

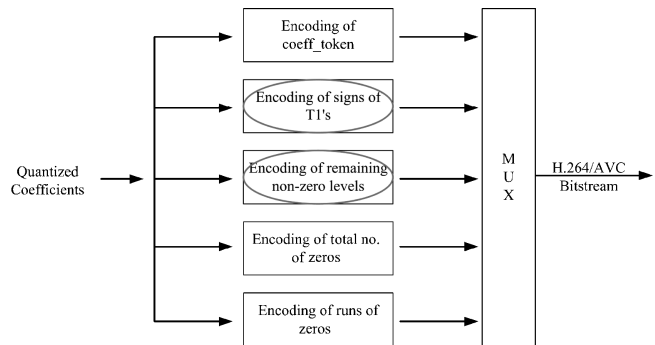


Fig. 4. Block diagram of CAVLC of H.264/AVC. Encircled syntax elements are used for SE-CAVLC.

321 its sign are encoded. Similar to MB header, header of 4×4
 322 block which includes coded block flag and significant map,
 323 should not be encrypted for the sake of bitstream compliance.
 324 Available encryption space (ES) which fulfills the above-
 325 mentioned conditions for SE-CAVLC and SE-CABAC is pre-
 326 sented in Sections III-A and III-B, respectively. Encryption
 327 and decryption of the protected bitstream are presented in
 328 Sections III-C and III-D, respectively.

329 A. ES for SE-CAVLC

330 In CAVLC, five syntax elements are used to code levels
 331 and runs as shown in Fig. 4. NZs are coded by three syntax
 332 elements, namely, *coeff_token*, signs of trailing ones, and
 333 remaining nonzero levels. Zeros are coded by two syntax
 334 elements, namely, total number of zeros and runs of zeros.
 335 A single syntax element, namely, *coeff_token* is used to code
 336 total NZs and number of trailing ones. It is followed by coding
 337 of signs of trailing ones (T1s). Remaining NZs are then coded
 338 using seven VLC look-up tables either by regular mode or by
 339 escape mode as explained in Section II-A1. They are mapped
 340 to some code from a specific VLC look-up table.

341 To keep the bitstream compliant, we cannot encrypt *coeff_*
 342 *token*, total number of zeros, and runs of zeros. Two
 343 syntax elements fulfill the above-mentioned conditions for
 344 encryptions. First is signs of trailing ones. Second is sign and
 345 magnitude of remaining NZs, both in regular and escape mode.
 346 For the sake of same bitrate, ES of SE-CAVLC consists of
 347 only those NZs whose VLC codewords have the same length.
 348 CAVLC uses multiple VLC tables with some threshold for
 349 incrementing the table as given in (2). Since the threshold for
 350 a specific table is highest possible value possible with that
 351 codeword length (this is the case when all the suffix bits of
 352 the codeword are 1), magnitude of encrypted NZ is such that
 353 VLC table transition is not affected. VLC codes, having same
 354 code length, constitute the ES. For VLC n table, ES is 2^n as
 355 given in (3). For table VLC0, every NZ has different codeword
 356 length, consequently we cannot encrypt the NZs in this table
 357 as follows:

$$TH[0 \dots 6] = (0, 2, 3, 6, 12, 24, 48, \infty). \quad (2)$$

$$ES[0 \dots 6] = (1, 2, 4, 8, 16, 32, 64, \infty). \quad (3)$$



Fig. 5. SE of binstrings in SE-CABAC.

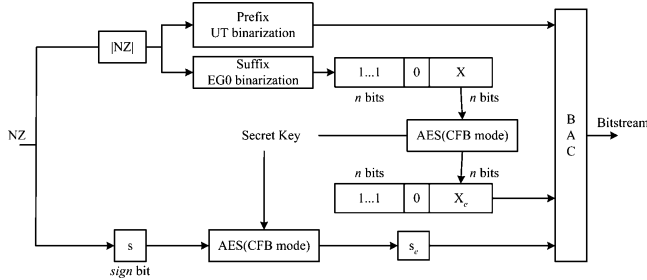


Fig. 6. Encryption process for NZs and their signs in CABAC of H.264/AVC.

B. ES for SE-CABAC

The main difference between SE-CAVLC and SE-CABAC is that in SE-CABAC, SE is not performed on CABAC bitstream. Rather it is performed on binstrings which are input to BAC as shown in Fig. 5. Among all the four binarization techniques, the unary and truncated unary codes have different code lengths for each input value as explained in Section II-A2. They do not fulfill the first condition and their encryption will change the bitrate of bitstream. Suffix of EGk and the fixed length code can be encrypted while keeping the bitrate unchanged. EGk is used for binarization of absolute value of levels and MVDs. Number of MVD binstrings have the same length and hence, first and second conditions are fulfilled. But owing to the fact that MVDs are part of MB header and are used for prediction of future motion vectors, their encryption does not fulfill third condition and their encryption makes the bitstream non-compliant. To conclude, the syntax elements which fulfill the criteria for encryption of H.264/AVC compliant bitstream are suffix of EG0 and sign bits of levels. Hence, for each NZ with $|NZ| > 14$, encryption is performed on $l(x)$ of EG0. It is followed by encryption of syntax element *coeff_sign_flag* which represents sign of levels of all nonzero levels. The fixed length code is used for binarization of syntax elements which belong to MB header and cannot be encrypted.

To keep the bitrate intact, ES for SE-CABAC consists of only those NZs whose EG0 binstrings have the same length as shown in Fig. 6. EG0 codes, having same code length, constitute the ES and it depends upon $\|NZ\|$. The ES is $2^{\log_2(n+1)}$ where n is the maximum possible value by suffix bits of EG0, i.e., when all the bits in suffix are 1.

C. SE of NZs in the Entropy Coding Stage of H.264/AVC

Let us consider $Y_i = X_i \oplus E_k(Y_{i-1})$ as the notation for the encryption of a n bit block X_i , using the secret key k with the AES cipher in CFB mode as given by (1), and performed as described in the scheme from Fig. 3. We have chosen to use this mode in order to keep the original compression rate. Indeed, with the CFB mode for each block, the size of the encrypted data Y_i can be exactly the same one as

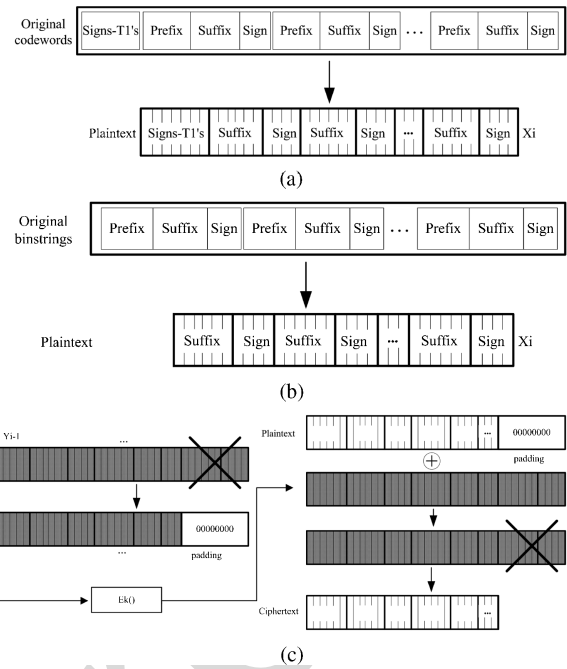


Fig. 7. (a) CAVLC plaintext. (b) CABAC plaintext. (c) Proposed SE scheme.

the size of the plaintext X_i . In this mode, the code from the previously encrypted block is used to encrypt the current one as shown in Fig. 3. The three stages of the proposed algorithm are the construction of the plaintext X_i , described in Section III-C1, the encryption of X_i to create Y_i which is provided in Section III-C2, and the substitution of the original codeword/binstring with the encrypted information, which is explained in Section III-C3. The overview of the proposed SE method is provided in Fig. 7.

1) *Construction of Plaintext*: As slices are independent coding units, SE should be performed on them independently. In case of SE-CAVLC, the plaintext is created by copying the encrypt-able bits from CAVLC bitstream to the vector X_i until either X_i is completely filled or slice-boundary comes as shown in Fig. 7(a). Let C , the length of the vector X_i , is 128. In case of SE-CABAC, we perform SE before BAC as shown in Fig. 7(b). In that case, we transform the non-binary syntax elements to binstrings through process of binarization and at the same time we fill the X_i with encrypted bits until either the vector X_i is completely filled or the slice boundary comes. The binarization of many syntax elements at the same time also makes the CABAC coding faster and increases its throughput [39]. Let $L(X_i)$ be the length up to which vector X_i is filled. In case of slice boundary, if $L(X_i) < C$, we apply a padding function $p(j) = 0$, where $j \in \{L(X_i) + 1, \dots, C\}$, to fill in the vector X_i with zeros up to C bits. Historically, padding was used to increase the security of the encryption, but in here it is used for rather technical reasons [28].

2) *Encryption of the Plaintext with AES in the CFB Mode*: In the encryption step with AES in the CFB mode, the previous encrypted block Y_{i-1} is used as the input of the AES algorithm in order to create Z_i . Then, the current plaintext X_i is XORed with Z_i in order to generate the encrypted text Y_i as given by (1). For the initialization, the initialization vector (IV)

is created from the secret key k according to the following strategy. The secret key k is used as the seed of the pseudo random number generator (PRNG). First, the secret key k is divided into 8 bits (byte) sequences. The PRNG produces a random number for each byte component of the key that defines the order of IV formation. Then, we substitute Y_0 with the IV, and Y_0 is used in AES to produce Z_1 . As illustrated in Fig. 7(c), with the CFB mode of the AES algorithm, the generation of the keystream Z_i depends on the previous encrypted block Y_{i-1} . Consequently, if two plaintexts are identical $X_i = X_j$ in the CFB mode, then always the two corresponding encrypted blocks are different, $Y_i \neq Y_j$.

3) *Substitution of the Original Bitstream*: The third step is the substitution of the original Y_i by the encrypted Y_i . For SE-CAVLC, CAVLC bitstream is accessed in sequential order as in the first step (construction of the plaintext X_i). Given the length in bits of each amplitude (S_n, S_{n-1}, \dots, S_1), we start substituting the original bits in the bitstream by the corresponding parts of Y_i as shown in Fig. 7. For SE-CABAC, binstrings are accessed in sequential order and we start substituting the original bits in them by the corresponding parts of Y_i as shown in Fig. 7. In case of slice boundaries, the total quantity of replaced bits is $L(X_i)$ and consequently we do not necessarily use all the bits of Y_i .

D. Decryption Process

The decryption process in the CFB mode works as follows. The previous block Y_{i-1} is used as the input to the AES algorithm in order to generate Z_i . By knowing the secret key k , we apply the same function $E_k(\cdot)$ as that used in the encryption stage. The difference is that the input of this process is now the ciphered vector. In case of SE-CAVLC, the ciphered vector is accessed in the sequential way in order to construct the plaintext Y_{i-1} which is then used in the AES to generate the keystream Z_i . The keystream Z_i is then XORed with the current block Y_i to generate X_i , as shown in Fig. 3(b). For SE-CAVLC, the resulting plaintext vector is split into segments in order to substitute the signs of trailing ones and suffixes (S_n, S_{n-1}, \dots, S_1) in the ciphered bitstream and to generate the original CAVLC bitstream. Afterward, we apply the entropy decoding and retrieve the quantized DCT coefficients. After the inverse quantization and the inverse DCT we get the decrypted and decoded video frame. In case of SE-CABAC, the difference is that binary arithmetic decoder is used to transform the SE-CABAC bitstream to encrypted binstrings which are then accessed to make the plaintext Y_{i-1} . The plaintext is decrypted and substituted back to generate original binstrings. They are then passed through inverse binarization, inverse quantization, and inverse DCT steps to get the decrypted and decoded video frame.

IV. EXPERIMENTAL RESULTS

In this section, we analyze the results for SE-CAVLC and SE-CABAC. We have used the reference implementation of H.264 JSVM 10.2 in AVC mode for video sequences in quarter common intermediate format (QCIF) and SD resolution. For the experimental results, nine benchmark video sequences

have been used for the analysis in QCIF format. Each of them represents different combinations of motion (fast/slow, pan/zoom/rotation), color (bright/dull), contrast (high/low), and objects (vehicle, buildings, people). The video sequences *Bus*, *City*, and *Foreman* contain camera motion while *Football* and *Soccer* contain camera panning and zooming along with object motion and texture in background. The video sequences *Harbour* and *Ice* contain high luminance images with smooth motion. *Mobile* sequence contains a complex still background and foreground motion.

In Section IV-A, we present an analysis of joint SE and H.264/AVC compression while in Section IV-B, we compare PSNR and quality when applying SE only on I frames and on I+P frames. In Section IV-C, security analysis, showing the efficiency of the proposed method, is developed.

A. Analysis of Joint SE and H.264/AVC Compression

We have applied simultaneously our SE and H.264/AVC compression as described in Section III, on all the benchmark video sequences. SE-CAVLC and SE-CABAC impart some characteristics to the bitstream. In spatial domain, SE video gets flat regions and change in pixel values mostly occur on MB boundaries. In temporal domain, *luma* and *chroma* values rise up to maximum limit and then come back to minimum values. This cycle keeps on repeating. Owing to this phenomenon, the pixel values change drastically in temporal domain. Lot of transitions are observed in values of color and brightness.

In a first set of experiments, we have analyzed the available ES in H.264/AVC bitstreams for both of SE-CAVLC and SE-CABAC. ES is defined as percentage of total bitstream size. MBs that contain many details and texture will have lot of NZs and, consequently, will be strongly encrypted. On the contrary, the homogeneous MBs, i.e., blocks that contain series of identical pixels, are less ciphered because they contain a lot of null coefficients which are represented by runs in CAVLC and by significant map in CABAC. In Table I, we provide ES for SE-CAVLC and SE-CABAC for different benchmark video sequences for quantization parameter (QP) value 18. While in Table II, ES for various QP values is shown for *Foreman* video sequence. Here the average number of bits available for SE per MB are also provided. One can note that ES is inversely proportional to QP value. When QP value is higher and implicitly the video compression is higher, we are able to encrypt fewer bits in the compressed frame. This is due to the fact that H.264/AVC has lesser number of NZs at higher QP values. From both these tables, it is evident that more ES is available for SE-CAVLC as compared to SE-CABAC. But ES is more affected by change in QP values for SE-CAVLC as compared to SE-CABAC. For example, for *Foreman* video sequence, ES varies from 28.55% to 6.70% for SE-CAVLC when QP varies from 12 to 42. For the same QP range, the change in ES for SE-CABAC is from 19.97% to 9.46% as shown in Table II. From Tables I and II, since PSNR of original H.264/AVC are very similar for both CAVLC and CABAC, in the rest of this section for the sake of comparison, we list only PSNR of CAVLC bitstreams.

TABLE I
ANALYSIS OF ES FOR SE FOR DIFFERENT BENCHMARK VIDEO
SEQUENCES AT QP VALUE 18

Sequence	SE-CAVLC		SE-CABAC	
	PSNR (dB)	ES (%)	PSNR (dB)	ES (%)
<i>Bus</i>	44.25	31.05	44.24	19.93
<i>City</i>	44.29	26.41	44.27	19.79
<i>Crew</i>	44.82	20.66	44.81	18.97
<i>Football</i>	44.61	25.33	44.59	19.45
<i>Foreman</i>	44.38	22.76	44.36	18.72
<i>Harbor</i>	44.10	30.49	44.09	20.01
<i>Ice</i>	46.47	24.64	46.46	17.72
<i>Mobile</i>	44.44	36.17	44.43	19.80
<i>Soccer</i>	44.27	23.42	44.21	19.94

TABLE II
ANALYSIS OF ES FOR SE OVER WHOLE RANGE OF QP VALUES FOR
Foreman VIDEO SEQUENCE

QP	SE-CAVLC		SE-CABAC	
	PSNR (dB)	ES (%)	PSNR (dB)	ES (%)
12	50.07	28.55	50.05	19.97
18	44.38	22.76	44.36	18.72
24	39.43	17.13	39.42	17.61
30	35.08	13.24	35.08	15.65
36	31.04	9.88	31.06	12.22
42	27.23	6.70	27.35	9.46

TABLE III
ANALYSIS OF INCREASE IN PROCESSING POWER FOR SE-CAVLC AND
SE-CABAC AT QP VALUE 18

Sequence	SE-CAVLC				SE-CABAC			
	Encoder		Decoder		Encoder		Decoder	
	I (%)	I+P (%)	I (%)	I+P (%)	I (%)	I+P (%)	I (%)	I+P (%)
<i>Bus</i>	0.69	0.31	3.77	2.7	0.57	0.25	3.37	2.3
<i>City</i>	0.5	0.26	3.36	2.4	0.44	0.23	3.06	2.1
<i>Crew</i>	0.31	0.15	2.52	1.5	0.29	0.14	2.22	1.2
<i>Football</i>	0.41	0.23	3.46	2.4	0.31	0.18	3.26	2.2
<i>Foreman</i>	0.47	0.23	3.19	2.2	0.41	0.20	2.99	2.0
<i>Harbor</i>	0.55	0.30	3.65	2.7	0.47	0.26	3.25	2.3
<i>Ice</i>	0.41	0.21	3.16	2.1	0.33	0.17	2.96	1.9
<i>Mobile</i>	0.76	0.35	4.33	3.3	0.72	0.33	4.03	3.0
<i>Soccer</i>	0.44	0.21	3.17	2.2	0.38	0.18	2.87	1.9

Table III gives a detailed overview of the required processing power for I and I+P video sequences at QP value 18. *Intra period* has been set 10 for I+P video sequences. One can observe that increase in computation time for encoder is less than 0.4% for both of SE-CAVLC and SE-CABAC while it is below than 3% for decoder for I+P sequence.

Fig. 8(a) and (b) shows the framewise analysis of increase in processing power for SE-CABAC at QP value 18 for *Foreman*. For experimentation, 2.1 GHz Intel Core 2 Duo T8100 machine with 3072 MB random access memory has been used. For I+P sequence encoding of 100 frames with *intra period* 10, it took 4372.5 s and 4381.3 s for CABAC and SE-CABAC, respectively. While it took 2.005 s and 2.045 s for CABAC and SE-CABAC decoding. It is a negligible increase in processing power and can be managed well even by handheld devices. It is important to note that increase in processing power of SE-

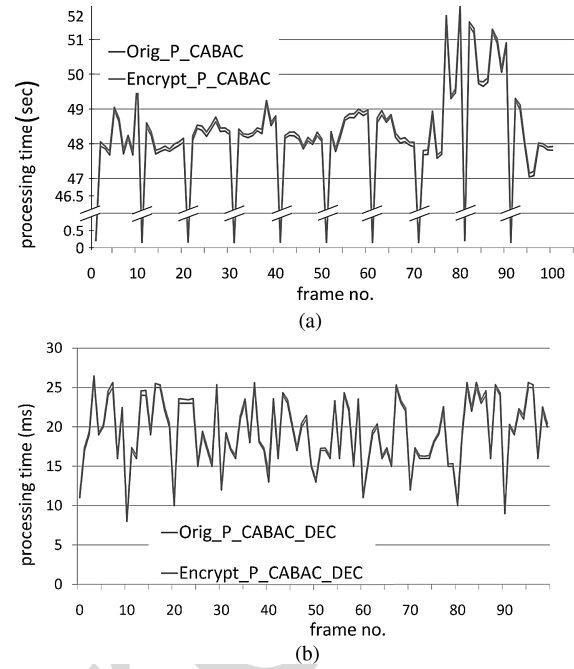


Fig. 8. Framewise time taken by SE-CABAC of *Foreman* video sequence for I+P frames at QP value 18 with *intra period* 10 during (a) encoding and (b) decoding.

CABAC is less than SE-CAVLC owing to two reasons. First, ES of SE-CABAC is lesser than that of SE-CAVLC as shown in Tables I and II. Second, CABAC takes lot more processing power than CAVLC. So increase in processing power because of encryption will be lower in terms of percentage. Thus, SE-CAVLC and SE-CABAC is possible in real-time along with compression.

B. PSNR and Quality of SE-CAVLC and SE-CABAC for I Frames and I+P Frames

Peak signal to noise ratio (PSNR) is widely used objective video quality metric. However, it does not perfectly correlate with a perceived visual quality due to nonlinear behavior of human visual system. Structural similarity index (SSIM) [33] takes into account the structural distortion measurement, since human vision system is highly specialized in extracting structural information from the viewing field. SSIM has a better correlation to the subjective impression. SSIM ranges from -1 to 1 . SSIM is 1 when both the images are the same. To present the visual protection of encrypted video sequences, PSNR and SSIM of I and I+P frames are presented.

1) *I Frames*: To demonstrate the efficiency of our proposed scheme, we have compressed 100 I frames of each sequence at 30 f/s. Figs. 9 and 10 show the encrypted first frame of *Foreman* video sequence at different QP values for SE-CAVLC and SE-CABAC, respectively. In H.264/AVC, blocks on the top array are predicted only from left while blocks on left are always predicted from top. Owing to this prediction, a band having width of 8 pixels at top of video frames can be observed for both of SE-CAVLC and SE-CABAC while this band has width of 4 pixels on left of video frames as shown in Figs. 9 and 10. The average PSNR values of *Foreman* is

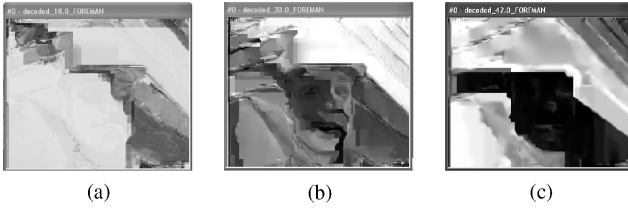


Fig. 9. Decoding of SE-CAVLC frame #1 of *Foreman* sequence with QP value equal to (a) 18, (b) 30, and (c) 42.

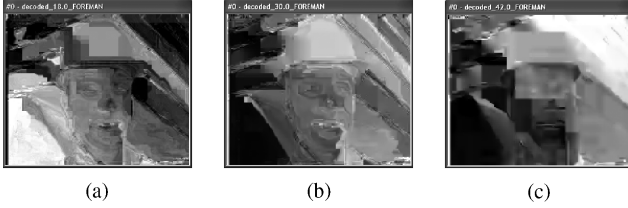


Fig. 10. Decoding of SE-CABAC frame #1 of *Foreman* sequence with QP value equal to (a) 18, (b) 30, and (c) 42.

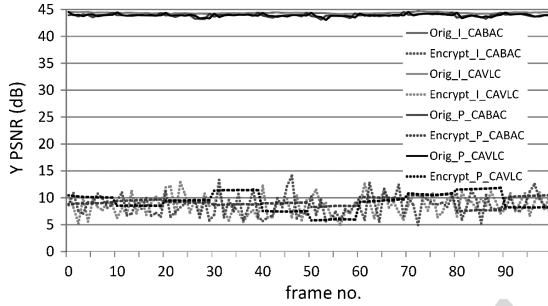


Fig. 11. Framewise PSNR of I and I+P frames for *Foreman* for SE-CAVLC and SE-CABAC at QP value 18.

589 given in Table IV over whole QP range. It is also compared
 590 with the PSNR obtained for the same video sequence without
 591 encryption. In Table IV, we present PSNR of original video
 592 only for CAVLC. PSNR for CABAC is very much similar as
 593 presented in Table I. One can note that whatever is the QP
 594 value, the quality of the encrypted video remains in the same
 595 lower range.

596 Table V compares the average PSNR of 100 I frames
 597 of all benchmark video sequences at QP value 18 without
 598 encryption and with SE. Average PSNR value of *luma* for
 599 all the sequences at QP value 18 is 9.49 dB for SE-CAVLC
 600 and 9.80 dB for SE-CABAC. It confirms that this algorithm
 601 works well for various combinations of motion, texture, and
 602 objects for I frames. It is also evident in framewise PSNR
 603 of *luma* of I frames of *Foreman* video sequence as shown in
 604 Fig. 11. Table VI contains the experimental results of SE of
 605 100 I frames for SD resolution. Here, average PSNR value of
 606 *luma* is 9.82 dB for SE-CAVLC and 9.83 dB for SE-CABAC,
 607 which is almost the same as that of QCIF resolution. It is
 608 evident that this algorithm is capable to encrypt high-quality
 609 information at all resolutions. For the rest of the section,
 610 we present analysis for QCIF resolution only, since more
 611 benchmark video sequences are available in this resolution.

612 Table VII shows the SSIM values of *luma* of benchmark
 613 video sequences without encryption and with SE. Results

TABLE IV
PSNR COMPARISON FOR I FRAMES WITHOUT ENCRYPTION AND WITH SE
FOR *Foreman* AT DIFFERENT QP VALUES

QP	PSNR (Y) (dB)			PSNR (U) (dB)			PSNR (V) (dB)		
	ORIG	SE	SE	ORIG	SE	SE	ORIG	SE	SE
		CAVLC	CABAC		CAVLC	CABAC		CAVLC	CABAC
12	50.1	8.6	8.4	50.0	19.8	24.1	50.8	9.6	22.6
18	44.4	8.7	8.6	45.7	24.1	24.4	47.6	10.2	22.1
24	39.4	8.7	8.7	41.9	26.4	24.4	44.2	24.9	22.8
30	35.1	9.4	8.7	39.8	27.4	24.6	41.4	25.4	23.6
36	31.0	9.4	8.5	37.7	28.1	24.9	38.6	24.8	23.2
42	27.2	9.4	8.7	36.2	25.5	24.9	36.9	24.6	24.0

TABLE V
PSNR COMPARISON FOR I FRAMES WITHOUT ENCRYPTION AND WITH SE
AT QP VALUE 18

Sequence	PSNR (Y) (dB)			PSNR (U) (dB)			PSNR (V) (dB)		
	ORIG	SE	SE	ORIG	SE	SE	ORIG	SE	SE
		CAVLC	CABAC		CAVLC	CABAC		CAVLC	CABAC
<i>Bus</i>	44.2	7.9	8.2	45.2	26.8	25.0	46.6	26.6	27.2
<i>City</i>	44.3	10.9	11.2	45.8	31.9	30.3	46.8	33.5	31.8
<i>Crew</i>	44.8	9.0	9.9	45.8	24.0	23.4	45.7	19.7	19.8
<i>Football</i>	44.6	11.5	11.5	45.8	14.9	14.4	46.0	24.3	23.6
<i>Foreman</i>	44.4	8.7	8.6	45.7	24.1	24.4	47.6	10.2	22.1
<i>Harbor</i>	44.1	9.2	9.5	45.6	27.1	24.6	46.7	33.2	31.3
<i>Ice</i>	46.5	10.6	10.4	48.8	24.3	25.6	49.3	16.9	20.4
<i>Mobile</i>	44.4	8.3	8.3	44.1	10.4	13.1	44.1	9.6	11.0
<i>Soccer</i>	44.3	9.3	10.6	46.6	22.1	19.7	47.9	28.2	24.4
Average	44.6	9.5	9.8	46.0	22.8	22.3	46.7	22.5	23.5

TABLE VI
PSNR COMPARISON FOR I FRAMES WITHOUT ENCRYPTION AND WITH SE
AT QP VALUE 18 (SD RESOLUTION)

Sequence	PSNR (Y) (dB)			PSNR (U) (dB)			PSNR (V) (dB)		
	ORIG	SE	SE	ORIG	SE	SE	ORIG	SE	SE
		CAVLC	CABAC		CAVLC	CABAC		CAVLC	CABAC
<i>City</i>	44.6	9.9	10.1	47.8	27.3	26.2	49.1	31.4	29.9
<i>Crew</i>	45.2	9.1	9.1	46.6	24.5	22.8	47.7	20.1	20.0
<i>Harbor</i>	44.5	9.4	9.4	47.5	22.9	22.9	48.7	28.8	26.8
<i>Ice</i>	46.2	10.7	10.4	51.5	27.8	27.8	52.0	25.0	26.0
<i>Soccer</i>	45.1	10.0	10.2	47.7	18.4	18.0	49.2	26.7	24.1
Average	45.1	9.8	9.8	48.2	24.2	23.5	49.4	26.4	25.4

614 verify the proposed scheme has distorted the structural in-
 615 formation present in the original video. Average SSIM value
 616 of video sequences without encryption is 0.993, while it is
 617 0.164 and 0.180 for SE-CAVLC and SE-CABAC, respectively.
 618 Fig. 12 shows the framewise SSIM of *luma* of *Foreman* video
 619 sequence for I frames. It is important to note SSIM value of
 620 complex video sequences is less than that of simple video
 621 sequences.

622 2) *I+P Frames*: Video data normally consists of an I frame
 623 and a trail of P frames. I frames are inserted periodically to
 624 restrict the drift because of lossy compression and rounding
 625 errors. In these experiments, *intra period* is set at 10 in a
 626 sequence of 100 frames. Results shown in Table VIII verify the
 627 effectiveness of our scheme over the whole range of QP values
 628 for *Foreman* video sequence. Table IX verifies the performance
 629 of our algorithm for all video sequences for I+P frames at
 630 QP value 18. Average PSNR of *luma* for all the sequences
 631 is 9.75 dB and 10.02 dB for SE-CAVLC and SE-CABAC,

TABLE VII
SSIM COMPARISON OF *luma* OF I FRAMES WITHOUT ENCRYPTION AND WITH SE AT QP VALUE 18

Sequence	CAVLC	SE-CAVLC	CABAC	SE-CABAC
<i>Bus</i>	0.995	0.069	0.994	0.064
<i>City</i>	0.994	0.115	0.994	0.093
<i>Crew</i>	0.991	0.184	0.991	0.153
<i>Football</i>	0.991	0.219	0.991	0.184
<i>Foreman</i>	0.990	0.198	0.990	0.165
<i>Harbor</i>	0.998	0.047	0.998	0.038
<i>Ice</i>	0.990	0.419	0.990	0.398
<i>Mobile</i>	0.998	0.040	0.998	0.356
<i>Soccer</i>	0.988	0.185	0.988	0.171
Average	0.993	0.164	0.993	0.180

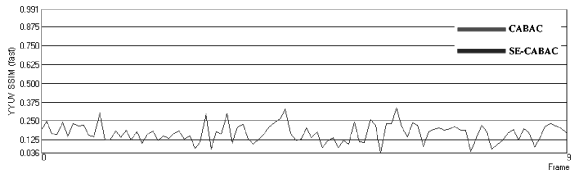


Fig. 12. Framewise SSIM of I frames for *Foreman* for SE-CABAC at QP value 18.

TABLE VIII
PSNR COMPARISON FOR I+P FRAMES WITHOUT ENCRYPTION AND WITH SE FOR *Foreman* AT DIFFERENT QP VALUES

Sequence	PSNR (Y) (dB)		PSNR (U) (dB)		PSNR (V) (dB)				
	ORIG	SE	ORIG	SE	ORIG	SE			
	CAVLC	CABAC	CAVLC	CABAC	CAVLC	CABAC			
12	49.6	8.7	8.1	49.9	18.4	23.0	50.6	10.4	21.6
18	43.9	9.1	10.4	45.5	23.6	23.9	47.6	8.0	23.2
24	38.9	9.6	9.7	42.0	26.9	24.9	44.3	25.8	25.0
30	34.6	9.2	9.2	39.8	28.6	24.9	41.5	26.6	24.0
36	30.7	10.1	8.2	37.9	28.4	24.3	38.8	22.8	23.3
42	27.0	9.4	8.6	36.3	26.5	26.8	36.9	25.6	24.6

632 respectively. Fig. 11 shows the framewise PSNR of *luma* of
 633 *Foreman* video sequence for I+P. Here, PSNR of SE-CAVLC
 634 and SE-CABAC remains almost the same for sequence of P
 635 frames and changes at every I frame, thus producing a staircase
 636 graph. SSIM quality metric has very low values and is not
 637 given here for the sake of brevity.

638 C. Security Analysis

639 1) *Analysis of Entropy and Local Standard Deviation:*
 640 The security of the encrypted image can be measured by
 641 considering the variations (local or global) in the protected
 642 image. Entropy is a statistical measure of randomness or
 643 disorder of a system which is mostly used to characterize the
 644 texture in the input images. Considering this, the information
 645 content of image can be measured with the entropy $H(X)$ and
 646 local standard deviation $\sigma(j)$. If an image has 2^k gray levels
 647 α_i with $0 \leq i \leq 2^k$ and the probability of gray level α_i is
 648 $P(\alpha_i)$, and without considering the correlation of gray levels,
 649 the first order entropy $H(X)$ is defined as follows:

$$H(X) = - \sum_{i=0}^{2^k-1} P(\alpha_i) \log_2(P(\alpha_i)). \quad (4)$$

TABLE IX
COMPARISON OF PSNR WITHOUT ENCRYPTION AND WITH SE FOR I+P FRAMES AT QP VALUE 18

Sequence	PSNR (Y) (dB)		PSNR (U) (dB)		PSNR (V) (dB)				
	ORIG	SE	ORIG	SE	ORIG	SE			
	CAVLC	CABAC	CAVLC	CABAC	CAVLC	CABAC			
<i>Bus</i>	43.7	7.6	7.7	45.1	27.2	25.4	46.4	24.7	27.0
<i>City</i>	43.8	11.4	11.1	45.7	32.5	30.2	46.8	32.5	31.7
<i>Crew</i>	44.5	9.0	10.0	45.8	25.1	22.0	45.7	19.6	20.2
<i>Football</i>	44.2	12.1	11.3	45.7	14.3	14.6	46.1	24.8	24.3
<i>Foreman</i>	43.9	9.1	10.4	45.5	23.6	23.9	47.6	8.0	23.2
<i>Harbor</i>	43.7	9.5	9.8	45.4	24.5	22.9	46.6	33.9	31.7
<i>Ice</i>	46.1	10.9	10.4	48.6	23.6	25.3	49.1	19.2	19.7
<i>Mobile</i>	43.8	8.4	8.8	44.2	10.1	12.5	44.1	9.6	11.8
<i>Soccer</i>	43.6	9.6	10.6	46.5	21.8	20.8	47.8	27.4	22.2
Average	44.2	9.75	10.0	45.8	22.5	21.9	46.7	22.2	23.5

If the probability of each gray level in the image is $P(\alpha_i) = \frac{1}{2^k}$, then the encryption of such image is robust against statistical attacks of first order, and thus $H(X) = \log_2(2^k) = k$ bits/pixel. In the image, the information redundancy r is defined as follows:

$$r = k - H(X). \quad (5)$$

Similarly, the local standard deviation $\sigma(j)$ for each pixel $p(j)$ taking account of its neighbors to calculate the local mean $\bar{p}(j)$, is given as follows:

$$\sigma(j) = \sqrt{\frac{1}{m} \sum_{i=1}^m (p(i) - \bar{p}(j))^2} \quad (6)$$

where m is the size of the pixel block to calculate the local mean and standard deviation, and $0 \leq j < M$, if M is the image size. In case of full encryption, entropy $H(X)$ is maximized with high values of local standard deviation. But in case of SE-CAVLC and SE-CABAC, the video frame is transformed to flat regions with blocking artifacts as depicted in Figs. 9 and 10. It is generally owing to variation in pixel values at MB boundaries. For all the benchmark sequences, the average information redundancy r for SE-CAVLC and SE-CABAC sequences is 0.94 and 0.55, respectively, while it is 1.11 for all the original sequences. Despite the fact that SE-CAVLC and SE-CABAC transform the video frames into flat region, the entropy of the encrypted video sequences from (4) is higher as compared to the original sequences. These flat regions are because of two reasons. First, flat regions are due to the fact that prediction is performed from edge pixels of neighboring MBs. Second, pixels have either very high value (bright video frame) or very low value (dark video frame) in SE video frame. This is owing to the fact that during reconstruction pixel value are clipped to 255 if they are greater than it and to 0 if they are below this lower range. So if many pixels have value beyond the upper or lower range, all of them will be clipped to the same value, thus creating a flat region which is either dark or bright. Based on this analysis, the statistical characteristics of SE-CAVLC and SE-CABAC bitstreams vary from full encryption systems.

From (6), we also analyzed the local standard deviation σ for each pixel while taking into account its neighbors.

TABLE X
STANDARD DEVIATION FOR SE OF *Foreman* VIDEO SEQUENCE AT
DIFFERENT QP VALUES

QP	CAVLC		CABAC	
	ORIG	SE-CAVLC	ORIG	SE-CABAC
12	6.75	71.49	7.02	69.69
18	7.21	73.23	7.53	59.97
24	8.57	91.98	8.63	84.55
30	6.35	35.99	6.71	57.87
36	6.90	47.42	6.93	68.04
42	7.91	75.26	8.11	71.17



Fig. 13. Key sensitivity test for encrypted frame #1 of *Foreman* video sequence for QP value 18. Encrypted frames are decrypted and decoded with (a) original key, (b) 1-bit different key (SE-CAVLC), and (c) 1-bit different key (SE-CABAC).

686 In Table X, the mean local standard deviation for *Foreman*
687 sequence at different QP values is given. For all benchmark
688 video sequences, the mean local standard deviation of *luma*
689 equals to 69.15 and 61.48 for the SE-CAVLC and SE-CABAC
690 bitstreams, respectively, where the mean local standard deviation
691 is less than ten gray levels for the original benchmark
692 sequences. One can note that local standard deviation of
693 encrypted sequences is higher than original sequences.

694 2) *Correlation of Adjacent Pixels*: Visual data is highly
695 correlated, i.e., pixels values are highly probable to repeat in
696 horizontal, vertical, and diagonal directions. A correlation of a
697 pixel with its neighboring pixel is then given by a tuple (x_i, y_i)
698 where y_i is the adjacent pixel of x_i . Since there is always three
699 directions in images, i.e., horizontal, vertical, and diagonal, so
700 we can define correlation direction between any two adjacent
701 pixels as follows:

$$corr_{(x,y)} = \frac{1}{n-1} \sum_0^n \left(\frac{x_i - \bar{x}_i}{\sigma_x} \right) \left(\frac{y_i - \bar{y}_i}{\sigma_y} \right) \quad (7)$$

702 where n represents the total number of tuples (x_i, y_i) , \bar{x}_i and
703 \bar{y}_i represent the local mean, and σ_x and σ_y represent the local
704 standard deviation, respectively.

705 Owing to the flat regions in SE-CAVLC and SE-CABAC
706 video sequences, the correlation values in these sequences will
707 be higher as compared to original image which contain texture
708 and edges. For all the benchmark sequences, the average
709 horizontal correlation coefficient is 0.88 and 0.87 for the SE-
710 CAVLC and SE-CABAC, respectively, while it is 0.80 for the
711 original sequences.

712 3) *Key Sensitivity Test*: Robustness against cryptanalyst
713 can be improved if the cryptosystem is highly sensitive toward
714 the key. The more the visual data is sensitive toward the key,
715 the more we would have data randomness. For this purpose, a
716 key sensitivity test is assumed where we pick one key and then
717 apply the proposed technique for encryption and then make a
718 1 bit change in the key and decode the bitstream. Numerical
719 results show that the proposed technique is highly sensitive
720 toward the key change, i.e., a different version of encrypted
721 video sequence is produced when the keys are changed, as
722 shown in Fig. 13. PSNR of *luma* of decrypted frames with 1-
723 bit different key is 10.39 dB and 8.31 dB for SE-CAVLC and
724 SE-CABAC as shown in Table XI. It lies in the same lower
725 range as decoded frames without decryption.

726 4) *Removal of Encrypted Data Attack*: In another ex-
727 periment, we have replaced the encrypted bits with constant
728 values in order to measure the strength of SE-CAVLC and SE-

TABLE XI

KEY SENSITIVITY TEST OF SE-CAVLC AND SE-CABAC ENCRYPTED
VIDEO FOR FRAME #1 *Foreman* VIDEO SEQUENCE FOR QP VALUE 18

	PSNR (Y) (dB)	PSNR (U) (dB)	PSNR (V) (dB)
Original key	44.60	45.73	47.35
SE-CAVLC (1-bit different key)	10.39	24.46	14.02
SE-CABAC (1-bit different key)	8.31	25.13	24.82

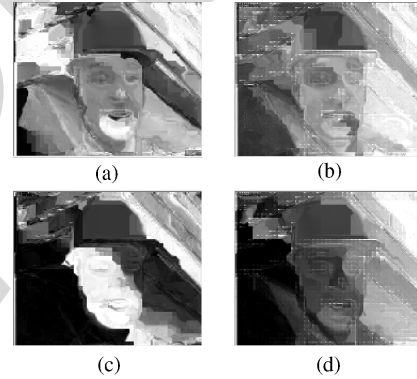


Fig. 14. Attack in the selectively encrypted image by removing the encrypted data. (a) SE-CAVLC encrypted image $\{Y, U, V\} = \{10.01, 26.86, 25.24\}$ dB. (b) SE-CAVLC attacked image $\{Y, U, V\} = \{8.87, 27.3, 26.3\}$ dB. (c) SE-CABAC encrypted image $\{Y, U, V\} = \{8.20, 17.95, 24.53\}$ dB. (d) SE-CABAC attacked image $\{Y, U, V\} = \{7.72, 28.6, 24.6\}$ dB.

729 CABAC proposed method as described in [27]. Here we have
730 used frame #1 of *Foreman* video sequence with QP value 24.
731 Fig. 14 shows both encrypted and attacked video frames for
732 SE-CAVLC and SE-CABAC. For example, Fig. 14(a) shows
733 SE-CAVLC video frame with PSNR = 10.01 dB for *luma*. If
734 we set the encrypted bits of all NZs to zero, we get the video
735 frame illustrated in Fig. 14(b) with *luma* PSNR = 8.87 dB.
736 Similarly, Fig. 14(c) shows SE-CABAC video frame having
737 PSNR = 8.20 dB while the attacked SE-CABAC video frame
738 has PSNR = 7.72 dB as shown in Fig. 14(d).

D. Comparative Evaluation

739 For the sake of comparative evaluation of our scheme, we
740 have compared it with six other recent techniques, which
741 include scrambling [9], NAL unit encryption [14], MB header
742 encryption [16], reversible ROI encryption [5], I frame en-
743 cryption [2], and multiple Huffman table permutation [36].
744 These techniques are different from each other in several
745

TABLE XII
COMPARISON OF PROPOSED SCHEME WITH OTHER RECENT METHODS

Video SE Scheme	Format Compliant	Robust to Transcoding	Domain	Bitrate Increase	Compression Independent	Encryption Algorithm
Scrambling for privacy protection [9]	Yes	No	Transform	Yes	Yes	Pseudo random sign inversion
NAL unit encryption [14]	No	No	Bitstream	No	No	Stream cipher
MB header data encryption [16]	No	No	Transform	No	No	Stream cipher
Reversible encryption of ROI [5]	Yes	Yes	Pixel	Yes	Yes	Pseudo random pixel permutations
I frame encryption [2]	No	No	Bitstream	No	No	AES
Multiple Huffman tables [36]	No	No	Bitstream	Yes	No	Huffman table permutations
Our scheme	Yes	No	Bitstream ^a	No	No	AES (CFB mode)

^aFor SE-CAVLC, bitstream is encrypted, while for SE-CABAC, binstrings are encrypted as explained in Section III-B.

746 aspects, e.g., working domain (pixel, transform, or bitstream)
 747 and encryption algorithm (pseudo random permutation, stream
 748 cipher, or AES). The comparison has been made based on
 749 several important characteristics of SE systems and is summa-
 750 rized in Table XII. Encryption algorithm used in SE scheme
 751 is of vital importance for the security level. AES has the
 752 highest security among all the known ciphers and our proposed
 753 scheme utilizes AES. Among the recent techniques, AES has
 754 been used only in [2] but their SE scheme is very naive and
 755 encrypts only I frames.

756 SE should not result in increase of bitrate. For example, if
 757 a video for 3G wireless connection has bitrate of 384 kb/s, its
 758 encrypted version should have the same bitrate. Otherwise, it
 759 cannot be played back on 3G connection. Our scheme keeps
 760 the bitrate intact. It is in contrast to other schemes which either
 761 allow increase in bitrate [5], [9], [36] or use stream cipher
 762 for the sake of same bitrate [14], [16], thus compromising on
 763 the security of the system.

764 Format compliance is another important aspect for en-
 765 crypted video data. Most of the schemes are not format
 766 complaint and their encrypted bitstreams cannot be decoded
 767 by reference decoder except SE schemes which work in pixel
 768 domain [5] and transform domain [9].

769 Our SE-CABAC scheme is the first format compliant tech-
 770 nique which is for arithmetic coding-based entropy coding
 771 module, while keeping the bitrate unchanged. Recent encryp-
 772 tion techniques for arithmetic coding [11], [13] are not format
 773 complaint and require lot of processing power.

774 To summarize, our proposed schemes (SE-CAVLC and
 775 SE-CABAC) meet all the requirements of an integrated
 776 compression-encryption system. Our proposed system is fully
 777 compliant to H.264/AVC decoder, with no change in bitrate
 778 and has the security of AES cipher.

779 V. CONCLUSION

780 In this paper, an efficient SE system has been proposed for
 781 H.264/AVC video codec for CAVLC and CABAC. The SE
 782 is performed in the entropy coding stage of the H.264/AVC
 783 using the AES encryption algorithm in the CFB mode. In
 784 this way, the proposed encryption method does not affect
 785 the bitrate and the H.264/AVC bitstream compliance. The SE
 786 is performed in CAVLC codewords and CABAC binstrings
 787 such that they remain a valid codewords/binstrings thereafter
 788 having exactly the same length. Experimental analysis has

789 been presented for I and P frames. The proposed scheme
 790 can be used for B frames without any modification, since B
 791 frames are also inter-frames but have bidirectional prediction.
 792 The proposed method has the advantage of being suitable for
 793 streaming over heterogeneous networks because of no change
 794 in bitrate. The experiments have shown that we can achieve
 795 the desired level of encryption, while maintaining the full
 796 bitstream compliance, under a minimal set of computational
 797 requirements. The presented security analysis confirmed a
 798 sufficient security level for multimedia applications in the
 799 context of SE. The proposed system can be extended for ROI-
 800 specific video protection [26] for video surveillance and can
 801 be applied to medical video transmission [24].

802 REFERENCES

803 [1] *Draft ITU-T Recommendation and Final Draft International Standard of*
 804 *Joint Video Specification (ITU-T Rec. H.264/ISO/IEC 14496-10 AVC)*,
 805 document JVT-G050, Joint Video Team (JVT), Mar. 2003.
 806 [2] M. Abomhara, O. Zakaria, O. Khalifa, A. Zaiden, and B. Zaiden, "En-
 807 hancing selective encryption for H.264/AVC using advanced encryption
 808 standard," *Int. J. Comput. Electric. Eng.*, vol. 2, no. 2, pp. 223–229,
 809 2010.
 810 [3] M. Bellare, T. Ristenpart, P. Rogaway, and T. Stegers, "Format-
 811 preserving encryption," in *Proc. 16th Annu. Int. Workshop Selected*
 812 *Areas Cryptography*, 2009, pp. 295–312.
 813 [4] G. Bjontegaard and K. Lillevold, *Context-Adaptive VLC Coding of*
 814 *Coefficients*, document JVT-C028, Joint Video Team, Fairfax, VA, May
 815 2002.
 816 [5] P. Carrillo, H. Kalva, and S. Magliveras, "Compression independent
 817 reversible encryption for privacy in video surveillance," *EURASIP J.*
 818 *Inform. Security*, vol. 2009, p. 13, 2009.
 819 [6] H. Cheng and X. Li, "Partial encryption of compressed images and
 820 videos," *IEEE Trans. Signal Process.*, vol. 48, no. 8, pp. 2439–2445,
 821 Aug. 2000.
 822 [7] J. Daemen and V. Rijmen, "AES proposal: The Rijndael clock cipher,"
 823 Proton World Int., Katholieke Univ. Leuven, ESAT-COSIC, Leuven,
 824 Belgium, Tech. Rep., 2002.
 825 [8] M. V. Droogenbroeck and R. Benedett, "Techniques for a selective
 826 encryption of uncompressed and compressed images," in *Proc. ACIVS*,
 827 Sep. 2002, pp. 90–97.
 828 [9] F. Dufaux and T. Ebrahimi, "Scrambling for privacy protection in video
 829 surveillance systems," *IEEE Trans. Circuits Syst. Video Technol.*, vol. 18,
 830 no. 8, pp. 1168–1174, Aug. 2008.
 831 [10] M. M. Fisch, H. Stgner, and A. Uhl, "Layered encryption techniques
 832 for DCT-coded visual data," in *Proc. 12th EUSIPCO*, Sep. 2004, pp.
 833 821–824.
 834 [11] M. Grangotto, E. Magli, and G. Olmo, "Multimedia selective encryption
 835 by means of randomized arithmetic coding," *IEEE Trans. Multimedia*,
 836 vol. 8, no. 5, pp. 905–917, Oct. 2006.
 837 [12] G. Jakimoski and K. Subbalakshmi, "Cryptanalysis of some multimedia
 838 encryption schemes," *IEEE Trans. Multimedia*, vol. 10, no. 3, pp.
 839 330–338, Apr. 2008.

- [13] W. Jiangtao, K. Hyungjin, and J. Villasenor, "Binary arithmetic coding with key-based interval splitting," *IEEE Signal Process. Lett.*, vol. 13, no. 2, pp. 69–72, Feb. 2006.
- [14] C. Li, X. Zhou, and Y. Zong, "NAL level encryption for scalable video coding," in *Proc. PCM*, no. 5353. 2008, pp. 496–505.
- [15] S. Lian, Z. Liu, Z. Ren, and Z. Wang, "Selective video encryption based on advanced video coding," in *Proc. PCM*, no. 3768. 2005, pp. 281–290.
- [16] S. Lian, Z. Liu, Z. Ren, and H. Wang, "Commutative encryption and watermarking in video compression," *IEEE Trans. Circuits Syst. Video Technol.*, vol. 17, no. 6, pp. 774–778, Jun. 2007.
- [17] E. Lin, A. Eskicioglu, R. Lagendijk, and E. Delp, "Advances in digital video content protection," *Proc. IEEE*, vol. 93, no. 1, pp. 171–183, Jan. 2005.
- [18] T. Lookabaugh and D. Sicker, "Selective encryption for consumer applications," *IEEE Commun. Mag.*, vol. 42, no. 5, pp. 124–129, May 2004.
- [19] R. Lukac and K. Plataniotis, "Bit-level based secret sharing for image encryption," *Patt. Recog.*, vol. 38, no. 5, pp. 767–772, May 2005.
- [20] D. Marpe, H. Schwarz, and T. Wiegand, "Context-based adaptive binary arithmetic coding in the H.264/AVC video compression standard," *IEEE Trans. Circuits Syst. Video Technol.*, vol. 13, no. 7, pp. 620–636, Jul. 2003.
- [21] K. Martin, R. Lukac, and K. Plataniotis, "Efficient encryption of wavelet-based coded color images," *Patt. Recog.*, vol. 38, no. 7, pp. 1111–1115, Jul. 2005.
- [22] I. Moccagatta and K. Ratakonda, *A Performance Comparison of CABAC and VCL-Based Entropy Coders for SD and HD Sequences*, document JVT-E079r2, Joint Video Team (JVT), Oct. 2002.
- [23] S. Ou, H. Chung, and W. Sung, "Improving the compression and encryption of images using FPGA-based cryptosystems," *Multimedia Tools Applicat.*, vol. 28, no. 1, pp. 5–22, Jan. 2006.
- [24] W. Puech and J. Rodrigues, "A new crypto-watermarking method for medical images safe transfer," in *Proc. 12th EUSIPCO*, 2004, pp. 1481–1484.
- [25] J.-M. Rodrigues, W. Puech, and A. Bors, "A selective encryption for heterogeneous color JPEG images based on VLC and AES stream cipher," in *Proc. Eur. Conf. CGIV*, Jun. 2006, pp. 34–39.
- [26] J.-M. Rodrigues, W. Puech, and A. Bors, "Selective encryption of human skin in JPEG images," in *Proc. IEEE Int. Conf. Image Process.*, Oct. 2006, pp. 1981–1984.
- [27] A. Said, "Measuring the strength of partial encryption scheme," in *Proc. IEEE Int. Conf. Image Process.*, vol. 2, Sep. 2005, pp. 1126–1129.
- [28] B. Schneier, *Applied Cryptography*. New York: Wiley, 1995.
- [29] Z. Shahid, M. Chaumont, and W. Puech, "Fast protection of H.264/AVC by selective encryption," in *Proc. SinFra IPAL Symp.*, Feb. 2009, pp. 11–21.
- [30] Z. Shahid, M. Chaumont, and W. Puech, "Fast protection of H.264/AVC by selective encryption of CABAC for I&P frames," in *Proc. 17th EUSIPCO*, Aug. 2009, pp. 2201–2205.
- [31] D. R. Stinson, *Cryptography: Theory and Practice (Discrete Mathematics and Its Applications)*. New York: Chapman and Hall/CRC Press, Nov. 2005.
- [32] L. Tang, "Methods for encrypting and decrypting MPEG video data efficiently," in *Proc. ACM Multimedia*, vol. 3, 1996, pp. 219–229.
- [33] Z. Wang, A. Bovik, H. Sheikh, and E. Simoncelli, "Image quality assessment: From error visibility to structural similarity," *IEEE Trans. Image Process.*, vol. 13, no. 4, pp. 600–612, Apr. 2004.
- [34] J. Wen, M. Severa, W. Zeng, M. Luttrell, and W. Jin, "A format-compliant configurable encryption framework for access control of video," *IEEE Trans. Circuits Syst. Video Technol.*, vol. 12, no. 6, pp. 545–557, Jun. 2002.
- [35] T. Wiegand, G. J. Sullivan, G. Bjontegaard, and A. Luthra, "Overview of the H.264/AVC video coding standard," *IEEE Trans. Circuits Syst. Video Technol.*, vol. 13, no. 7, pp. 560–576, Jul. 2003.
- [36] C.-P. Wu and C.-C. Kuo, "Design of integrated multimedia compression and encryption systems," *IEEE Trans. Multimedia*, vol. 7, no. 5, pp. 828–839, Oct. 2005.
- [37] K. Yabuta, H. Kitazawa, and T. Tanaka, "A new concept of security camera monitoring with privacy protection by masking moving objects," in *Proc. Adv. Multimedia Inform. Process.*, vol. 1, no. 3767. 2005, pp. 831–842.
- [38] W. Zeng and S. Lei, "Efficient frequency domain selective scrambling of digital video," *IEEE Trans. Multimedia*, vol. 5, no. 1, pp. 118–129, Mar. 2003.
- [39] S. Ziauddin, I. U. Haq, and M. A. Khan, "Method and system for fast context based adaptive binary arithmetic coding," U.S. Patent 7 221 296, 2007.



Zafar Shahid received the B.S. degree in electrical engineering from the University of Engineering and Technology, Lahore, Pakistan, and the M.S. degree in image processing from the National Institute of Applied Sciences, Lyon, France, in 2001 and 2007, respectively. Currently, he is a Ph.D. student at the Laboratory of Computer Science, Robotics, and Microelectronics, University of Montpellier II, Montpellier, France.

Before his M.S. degree, he was a Senior Embedded System Engineer with Streaming Networks, Santa Clara, CA, where he was involved in the research and development in the domain of video processing. His current research interests include compression, watermarking, and encryption of scalable video.



Marc Chaumont was born in November 1976, in France. He received the Engineering Diploma degree from the National Institute of Applied Sciences (INSA), Rennes, France, in 1999, and the Ph.D. degree from the IRISA Rennes (INRIA, CNRS, University of Rennes 2, and INSA) in 2003, both in computer sciences.

His Ph.D. thesis was about video objects representations, with dynamic coding and scalability functionalities, in the video compression area. He has carried on research activities for one year at the INRIA Rennes and for another year at the University Technological Institute, Bayonne, France, as a Visiting Assistant Professor. During this last year, he focused on face tracking using a deformable 3-D face model. Since September 2005, he is an Assistant Professor with the Laboratory of Computer Science, Robotics, and Microelectronics, Montpellier, France, and the University of Nîmes, Nîmes, France. His current research interests include watermarking, steganography, video compression, and to a lesser extent segmentation and tracking in videos.



William Puech (M'XX) received the Diploma degree in electrical engineering from the University of Montpellier, Montpellier, France, in 1991, and the Ph.D. degree in signal-image-speech from the Polytechnic National Institute, Grenoble, France, in 1997.

He started his research activities in image processing and computer vision. He was a Visiting Research Associate with the University of Thessaloniki, Thessaloniki, Greece. From 1997 to 2000, he was an Assistant Professor with the University of Toulon, Toulon, France, with research interests including methods of active contours applied to medical images sequences. Between 2000 and 2008, he was an Associate Professor and since 2009, he has been a Full Professor of image processing with the Laboratory of Computer Science, Robotics, and Microelectronics, University of Montpellier. He has developed applications on medical images, cultural heritage, and video surveillance. He is the Head of the ICAR Team (Image and Interaction), University of Montpellier. He has published more than 12 journal papers, 4 book chapters, and more than 65 conference papers. His current research interests include the areas of protection of visual data (image, video, and 3-D object) for safe transfer by combining watermarking, data hiding, compression, and cryptography.

Prof. Puech is a reviewer for more than 15 journals (IEEE TRANSACTIONS ON IMAGE PROCESSING, IEEE TRANSACTIONS ON MULTIMEDIA, *Signal Processing: Image Communication*, *Journal of Applied Signal Processing*, *Journal of Electronic Imaging*, and others) and more than ten conference proceedings (IEEE ICIP, EUSIPCO, WIAMIS, IWDW, and others). He is currently a member of SPIE. Since 2005, he has been in the Technical Program Committee of EUSIPCO, and since 2009, he has been in the Area Chair "Image and Multidimensional Signal Processing" of EUSIPCO.

914
915
916
917
918
919
920
921
922
923
924
925
926
927
928
929
930
931
932
933
934
935
936
937
938
939
940
941
942
943
944
945
946
947
948
949
950
951
952
953
954
955
956
957
958
959
960
961
962
963
964
965
966
967
968
969
970
971
972
973
974
975
976
977
978
979

AUTHOR QUERIES

AUTHOR PLEASE ANSWER ALL QUERIES

- 980
981 AQ:1= Please provide the expanded form of NZs.
982 AQ:2= Please provide the expanded form of AC and DC.
983 AQ:3= Please provide the expanded form of SD.
984 AQ:4= Please verify the volume no. in Ref. [5].
985 AQ:5= Please provide the issue no. or month in Ref. [5].
986 AQ:6= Please provide the technical report no. in Ref. [7].
987 AQ:7= Please provide the membership year of Puech.
988 AQ:8= Please verify the sense of the sentence "...he has been in the Area Chair..."
- 989 END OF ALL QUERIES

IEEE PROOF